Journée d'hommage au Prof. Biarez

MODELLING OF LANDSLIDES AS A BIFURCATION PROBLEM

F. DARVE, F. PRUNIER, S. LIGNON, L. SCHOLTES, J. DURIEZ
Laboratoire Sols, Solides, Structures, INPG-UJF-CNRS, Grenoble, France –ALERT, RNVO, DIGA, LESSLOSS, SIGMA, STABROCK
F. NICOT
CEMAGREF Grenoble, ALERT, RNVO
F. LAOUAFA
INERIS, Paris, France

I Introduction

1 Failure : the classical view

2 An example of diffuse failure strictly inside Mohr-Coulomb limit surface

3 Hill’s sufficient condition of stability and bifurcation criteria : phenomenological analyses for axisymmetric and plane strain conditions

4 A multiscale analysis of instabilities with a micromechanical model

5 A direct numerical analysis of instabilities with a discrete element method

II Landslides modelling : Trévoux and Petacciato examples

III Rockfalls modelling : Acropolis example

IV Loading paths with constant q

I Introduction

FAILURE : THE CLASSICAL VIEW

- Rate independent materials :

$$d\boldsymbol{\sigma} = \mathbf{F}(d\boldsymbol{\varepsilon})$$

$$\forall \lambda \geq 0 : \mathbf{F}(\lambda d\boldsymbol{\varepsilon}) \equiv \lambda \mathbf{F}(d\boldsymbol{\varepsilon}) \Rightarrow$$ **F** Homogeneous of degree 1

- Euler's identity :

$$d\boldsymbol{\sigma} = \mathbf{F}(d\boldsymbol{\varepsilon}) \equiv \frac{\partial \mathbf{F}}{\partial(d\boldsymbol{\varepsilon})} d\boldsymbol{\varepsilon} \qquad d\boldsymbol{\sigma} = \mathbf{M}_h(\mathbf{v}) d\boldsymbol{\varepsilon} \quad \left(\mathbf{v} = \frac{d\boldsymbol{\varepsilon}}{\|d\boldsymbol{\varepsilon}\|} \right)$$

$$d\sigma_\alpha = M_{\alpha\beta}\, d\varepsilon_\beta$$

- Perfect plasticity :

$$d\boldsymbol{\sigma} = 0$$ and $$\|d\boldsymbol{\varepsilon}\| \neq 0$$ (Limit stress state)

$$\Rightarrow \quad \begin{cases} \det \mathbf{M}_h = 0 \\ \mathbf{M}_h\, d\boldsymbol{\varepsilon} = 0 \end{cases}$$

Plastic limit condition
Plastic flow rule

UNDRAINED LOADING ON LOOSE SANDS

Typical behaviour of a loose sand : undrained (isochoric) triaxial compression

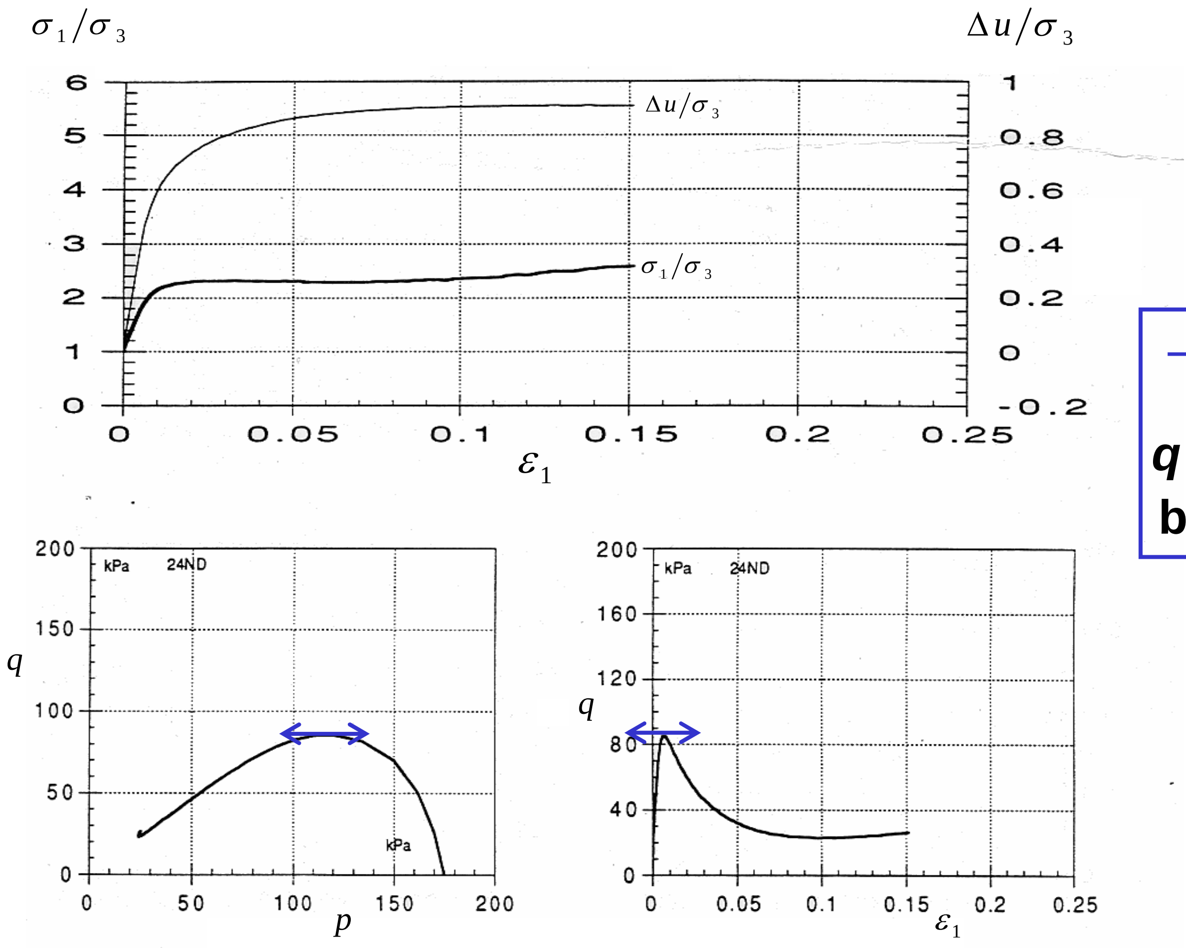

→ Experimental evidence :

***q* goes through a maximum before Mohr-Coulomb limit**

UNDRAINED LOADING ON LOOSE SANDS

Experimental observations (I. Georgopoulos, J. Desrues – Grenoble, DIGA project):

Partial diffuse failure

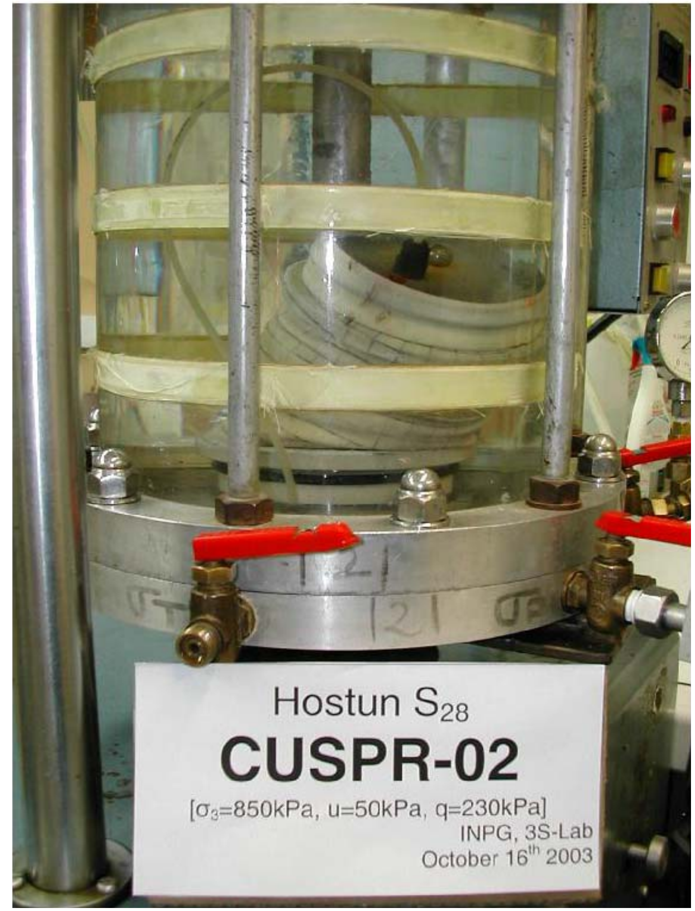

Total diffuse failure

UNDRAINED LOADING ON LOOSE SANDS

A typical example of a diffuse mode of failure :

- $\boxed{\Delta q = \Delta F / S}$: *« small » additional force (stress controlled loading)*

  q peak is unstable according to LYAPUNOV definition

  Non-controllability after R. NOVA definition

- *Second order work criterion :*

$$\boxed{\begin{aligned} d^2W &= d\sigma_1 d\varepsilon_1 + 2d\sigma_3 d\varepsilon_3 \\ &= dq d\varepsilon_1 \quad {}^{(1)} \end{aligned}}$$

(1) with the isochoric condition : $d\varepsilon_v = 0$

After HILL condition of stability, *q* peak is unstable

- *For axisymmetric conditions* :

$$\boxed{\begin{bmatrix} dq \\ d\varepsilon_v \end{bmatrix} = \mathbf{N} \begin{bmatrix} d\varepsilon_1 \\ d\sigma_3 \end{bmatrix}}$$

- Undrained loading : $d\varepsilon_v = 0$
- At *q* peak : *dq* = 0
- Bifurcation criterion : det **N** = 0
- Failure rule : $\boxed{\mathbf{N} \begin{bmatrix} d\varepsilon_1 \\ d\sigma_3 \end{bmatrix} = \begin{bmatrix} 0 \\ 0 \end{bmatrix}}$

Conclusions : ***q* peak is a proper failure state, strictly inside the plastic limit condition, without localization pattern, properly described by Hill's condition and a bifurcation criterion**

HILL'S CONDITION OF STABILITY

- DRUCKER's postulate

$\forall\ d\sigma, d\varepsilon^{p}\ :\ d^2W^{p} = d\sigma : d\varepsilon^{p} > 0$

always satisfied in associated elasto-plasticity

$d\varepsilon^{p} = d\lambda\,(df/d\sigma) \Rightarrow d^2W^{p} = \underbrace{d\lambda}_{>0}\,(\underbrace{d\sigma : df/d\sigma}_{>0})$

- HILL's condition of stability

$\forall\ d\sigma, d\varepsilon\ :\ d^2W = d\sigma : d\varepsilon > 0$ DRUCKER $\Rightarrow$ HILL

Incrementally linear constitutive relations

$d\sigma = \mathbf{M}\,d\varepsilon \qquad d^2W = {}^t d\varepsilon\,\mathbf{M}\,d\varepsilon = {}^t d\varepsilon\,\mathbf{M}^s\,d\varepsilon \longrightarrow d^2W > 0 \Leftrightarrow \det \mathbf{M}^s > 0$

- Associated elasto-plasticity : $\mathbf{M} \equiv \mathbf{M}^s$

plasticity limit condition : $\det \mathbf{M} = 0$

stability condition : $\det \mathbf{M}^s = 0$ IDENTICAL !

- Non-associated elasto-plasticity :

$\det \mathbf{M}^s$ is always vanishing before $\det \mathbf{M}$ and $\det {}^t n \mathbf{L} n = 0$,
$\Rightarrow \det \mathbf{M}^s = 0$ is satisfied stricly inside the plastic limit condition and,
inside the localisation condition

CONSTITUTIVE RELATIONS

$$\mathbf{d\varepsilon} = \mathbf{M(u)d\sigma} = \mathbf{M}^1\mathbf{d\sigma} + \frac{1}{\|\mathbf{d\sigma}\|}\mathbf{M}^2\mathbf{d\sigma}\,\mathbf{d\sigma} + \cdots$$

Incrementally non-linear relations of second order :

$$d\varepsilon_{ij} = M^1_{ijkl}d\sigma_{kl} + \frac{1}{\|\mathbf{d\sigma}\|}M^2_{ijklmn}d\sigma_{kl}d\sigma_{mn}$$

In fixed stress-strain principal axes :

Incrementally non-linear model (quadratic interpolation) :

$$\begin{pmatrix} d\varepsilon_1 \\ d\varepsilon_2 \\ d\varepsilon_3 \end{pmatrix} = \frac{1}{2}\left[\mathbf{N}^+ + \mathbf{N}^-\right]\cdot\begin{pmatrix} d\sigma_1 \\ d\sigma_2 \\ d\sigma_3 \end{pmatrix} + \frac{1}{2\|\mathbf{d\sigma}\|}\left[\mathbf{N}^+ - \mathbf{N}^-\right]\cdot\begin{pmatrix} (d\sigma_1)^2 \\ (d\sigma_2)^2 \\ (d\sigma_3)^2 \end{pmatrix}$$

Octo-linear model (linear interpolation) :

$$\begin{pmatrix} d\varepsilon_1 \\ d\varepsilon_2 \\ d\varepsilon_3 \end{pmatrix} = \frac{1}{2}\left[\mathbf{N}^+ + \mathbf{N}^-\right]\cdot\begin{pmatrix} d\sigma_1 \\ d\sigma_2 \\ d\sigma_3 \end{pmatrix} + \frac{1}{2}\left[\mathbf{N}^+ - \mathbf{N}^-\right]\cdot\begin{pmatrix} |d\sigma_1| \\ |d\sigma_2| \\ |d\sigma_3| \end{pmatrix}$$

Constitutive matrices $\mathbf{N}^+$ and $\mathbf{N}^-$:

$$E_i = \left(\frac{\partial\sigma_i}{\partial\varepsilon_i}\right)_{\sigma_j,\sigma_k}, \quad \upsilon_i^j = -\left(\frac{\partial\varepsilon_j}{\partial\varepsilon_i}\right)_{\sigma_j,\sigma_k}$$

$$\mathbf{N}^+ = \begin{bmatrix} \frac{1}{E_1^+} & -\frac{\upsilon_2^{1+}}{E_2^+} & -\frac{\upsilon_3^{1+}}{E_3^+} \\ -\frac{\upsilon_1^{2+}}{E_1^+} & \frac{1}{E_2^+} & -\frac{\upsilon_3^{2+}}{E_3^+} \\ -\frac{\upsilon_1^{3+}}{E_1^+} & -\frac{\upsilon_2^{3+}}{E_2^+} & \frac{1}{E_3^+} \end{bmatrix} \quad \mathbf{N}^- = \begin{bmatrix} \frac{1}{E_1^-} & -\frac{\upsilon_2^{1-}}{E_2^-} & -\frac{\upsilon_3^{1-}}{E_3^-} \\ -\frac{\upsilon_1^{2-}}{E_1^-} & \frac{1}{E_2^-} & -\frac{\upsilon_3^{2-}}{E_3^-} \\ -\frac{\upsilon_1^{3-}}{E_1^-} & -\frac{\upsilon_2^{3-}}{E_2^-} & \frac{1}{E_3^-} \end{bmatrix}$$

(+) for compression,
(-) for extension

Six generalized triaxial loading paths : $(d\sigma_1, d\sigma_2, d\sigma_3) = (\pm1,0,0);(0,\pm1,0);(0,0,\pm1)$

BIFURCATION ANALYSIS IN AXISYMMETRIC CONDITIONS

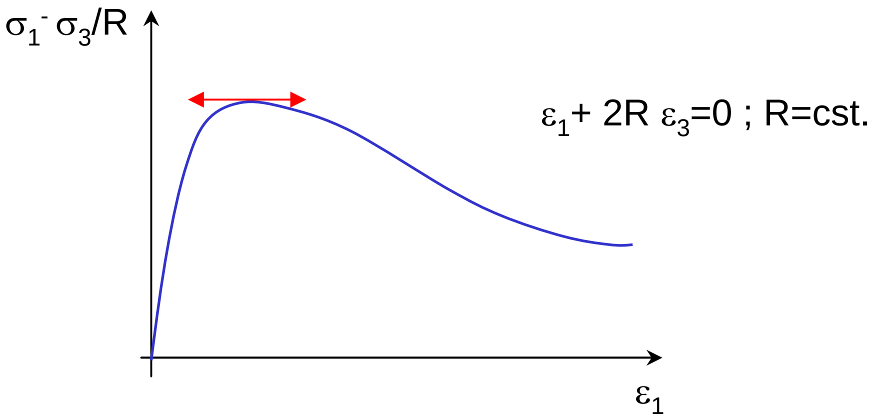

- $(\sigma_1 - \sigma_3/R)$ peak is unstable according to LYAPUNOV
- $d^2W = d\sigma_1 d\varepsilon_1 + 2\, d\sigma_3 d\varepsilon_3 = (d\sigma_1 - d\sigma_3/R)\, d\varepsilon_1 \leq 0$ from $(\sigma_1 - \sigma_3/R)$ peak
- $$\begin{bmatrix} d\sigma_1 - d\sigma_3/R \\ d\varepsilon_1 + 2R\, d\varepsilon_3 \end{bmatrix} = \mathbf{Q} \begin{bmatrix} d\varepsilon_1 \\ d\sigma_3/R \end{bmatrix}$$

At $(\sigma_1 - \sigma_3/R)$ peak : $\begin{bmatrix} 0 \\ 0 \end{bmatrix} = \mathbf{Q} \begin{bmatrix} d\varepsilon_1 \\ d\sigma_3/R \end{bmatrix}$

BIFURCATION CRITERION :

$$\det \mathbf{Q} = 0 \Leftrightarrow 2\, E_1^{-}/E_3^{-}(1-\nu_3^{3-})R^2 - 2(\nu_1^{3-} + E_1^{-}\, \nu_3^{1-}/E_3^{-})R + 1 = 0$$

$$\Delta = -(2/(E_3^{-})^2)\, \det \mathbf{M}^s \geq 0$$

Loss of controllability after NOVA (1994)

First unstable direction : $$\frac{d\sigma_1}{\sqrt{2}\, d\sigma_3} = \frac{E_1^{-}}{\sqrt{2}\, E_3^{-}} \; \frac{(1-\nu_3^{3-})(E_1^{-}\, \nu_3^{1-} - E_3^{-}\, \nu_1^{3-})}{E_1^{-}(1-\nu_3^{3-}) - \nu_1^{3-}(E_1^{-}\, \nu_3^{1-} - E_3^{-}\, \nu_1^{3-})}$$

Rupture rule : $E_1^{-}\, d\varepsilon_1 + (2\, \nu_3^{1-}\, E_1^{-}/E_3^{-} - 1/R)\, d\sigma_3 = 0$

BIFURCATION ANALYSIS IN PLANE STRAIN CONDITIONS (H.D.V. KHOA)

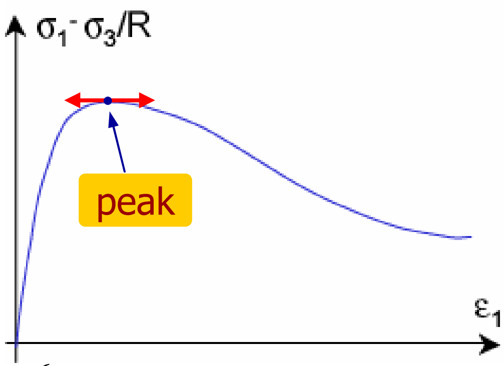

$$\begin{cases} d\varepsilon_1 = \text{ positive constant} \\ d\varepsilon_2 = 0 \\ d\varepsilon_1 + R d\varepsilon_3 = 0 \text{ (R=cst.)} \end{cases}$$

- **Second order work:**

$$\begin{aligned} d^2W &= d\sigma_1 d\varepsilon_1 + d\sigma_3 d\varepsilon_3 \\ &= \left(d\sigma_1 - d\sigma_3/R\right)d\varepsilon_1 + d\sigma_3\left(d\varepsilon_1 + R d\varepsilon_3\right)/R \\ &= \left(d\sigma_1 - d\sigma_3/R\right)d\varepsilon_1 \leq 0 \quad \text{from} \quad \left(\sigma_1 - \sigma_3/R\right) \text{ peak} \end{aligned}$$

$\Rightarrow$ The peak is potentially unstable in Hill's sense

- **Octo-linear model:** $\begin{bmatrix} d\sigma_1 - d\sigma_3/R \\ d\varepsilon_1 + R d\varepsilon_3 \end{bmatrix} = \underline{\underline{Q}} \begin{bmatrix} d\varepsilon_1 \\ d\sigma_3/R \end{bmatrix}$

$\det \underline{\underline{Q}} = 0$ → Bifurcation criterion

$$\Leftrightarrow E_1^-\left(1 - V_2^{3-}V_3^{2-}\right)R^2 - \left[E_3^-\left(V_1^{3-} + V_1^{2-}V_2^{3-}\right) + E_1^-\left(V_3^{1-} + V_3^{2-}V_2^{1-}\right)\right]R + E_3^-\left(1 - V_1^{2-}V_2^{1-}\right) = 0$$

$$\Delta = -4\left(E_1^-\right)^2\left(E_3^-\right)^2 \det \underline{\underline{P}}^S \geq 0 \qquad \left(\begin{bmatrix} d\varepsilon_1 \\ d\varepsilon_3 \end{bmatrix} = \underline{\underline{P}} \begin{bmatrix} d\sigma_1 \\ d\sigma_3 \end{bmatrix}\right)$$

$\det \underline{\underline{P}}^s = 0$ → First bifurcation point

→ First bifurcation direction

$$\left(\frac{d\sigma_1}{d\sigma_3}\right)_c = \frac{E_1^-\left(1 - V_2^{3-}V_3^{2-}\right)\left[E_1^-\left(V_3^{1-} + V_3^{2-}V_2^{1-}\right) - E_3^-\left(V_1^{3-} + V_1^{2-}V_2^{3-}\right)\right]}{E_3^-\left[E_1^-\left(D + \left(1 - V_1^{2-}V_2^{1-}\right)\left(1 - V_2^{3-}V_3^{2-}\right)\right) - E_3^-\left(V_1^{3-} + V_1^{2-}V_2^{3-}\right)^2\right]}$$

AXISYMMETRIC PROPORTIONAL STRAIN PATHS – INL2 model, DENSE SAND

R $\in$ (0.3, 0.35, 0.4, 0.45, 0.5, 0.6, 0.7, 0.8, 0.9, 1.0)

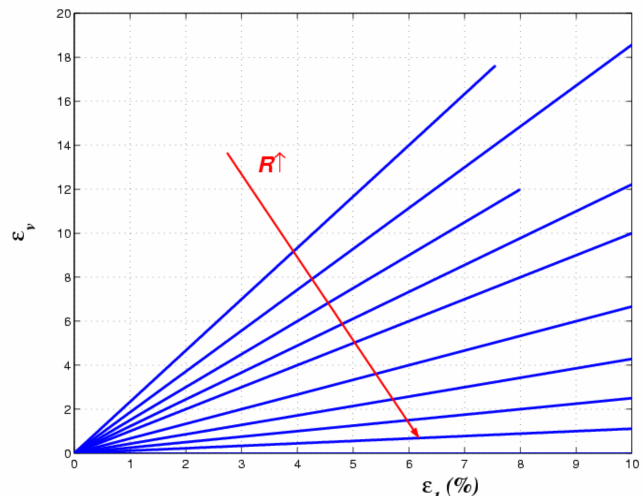

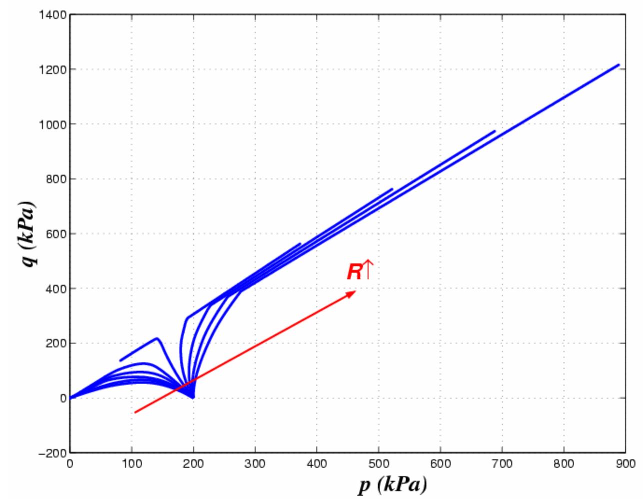

Volumetric strain versus axial strain on the left and deviatoric stress versus mean pressure on the right

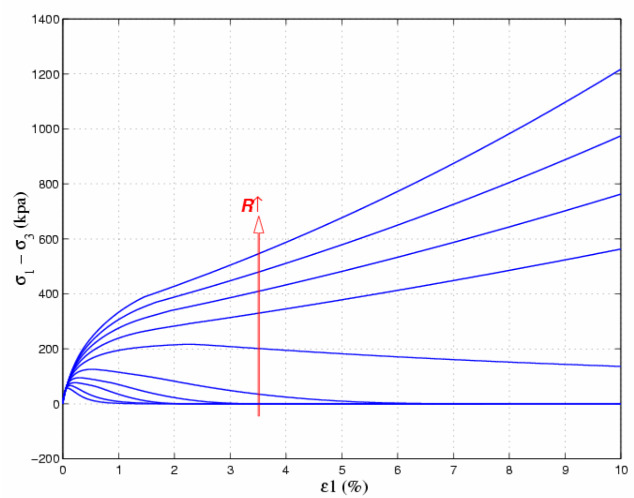

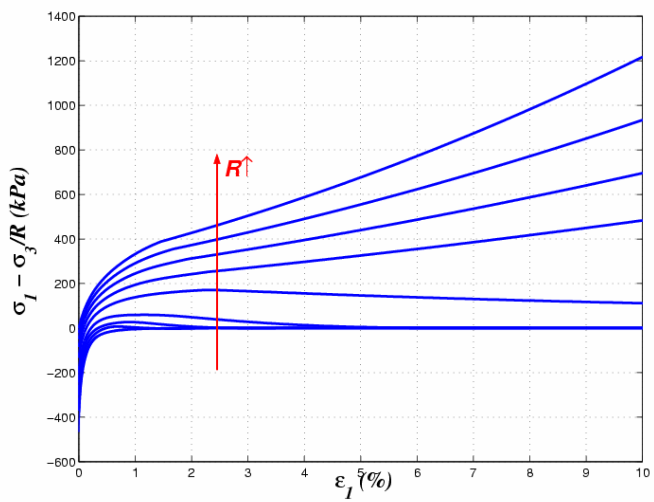

Deviatoric stress versus axial strain on the left and (σ_1-σ_3/R) versus axial strain on the right

PLANE STRAIN PROPORTIONAL STRAIN PATHS (H.D.V. KHOA)

octo-linear model

- Loose Hostun sand ⇒ liquefaction for all R values

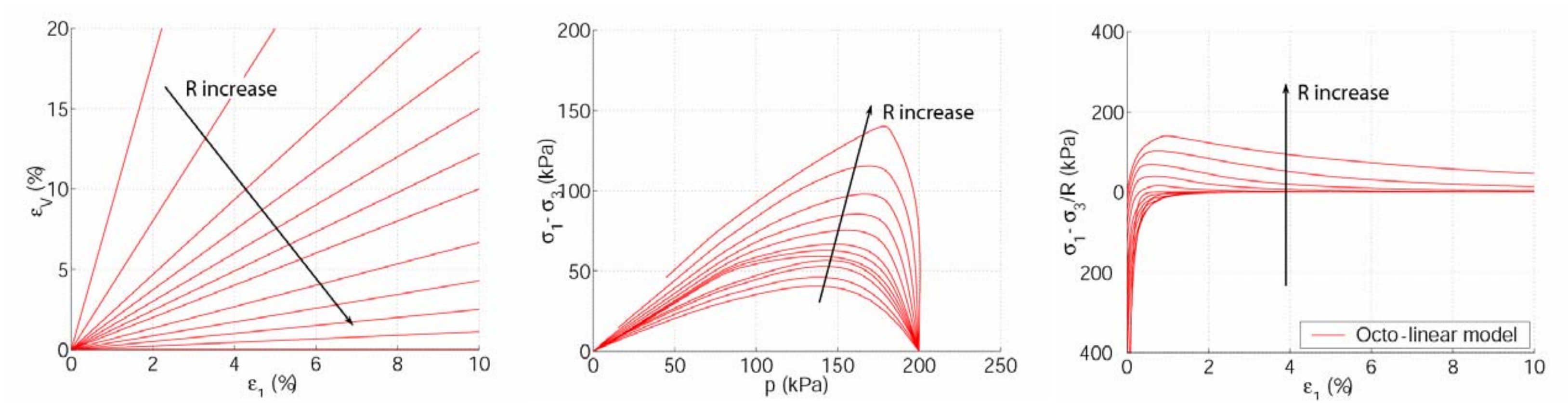

- Dense Hostun sand ⇒ liquefaction for only low R values

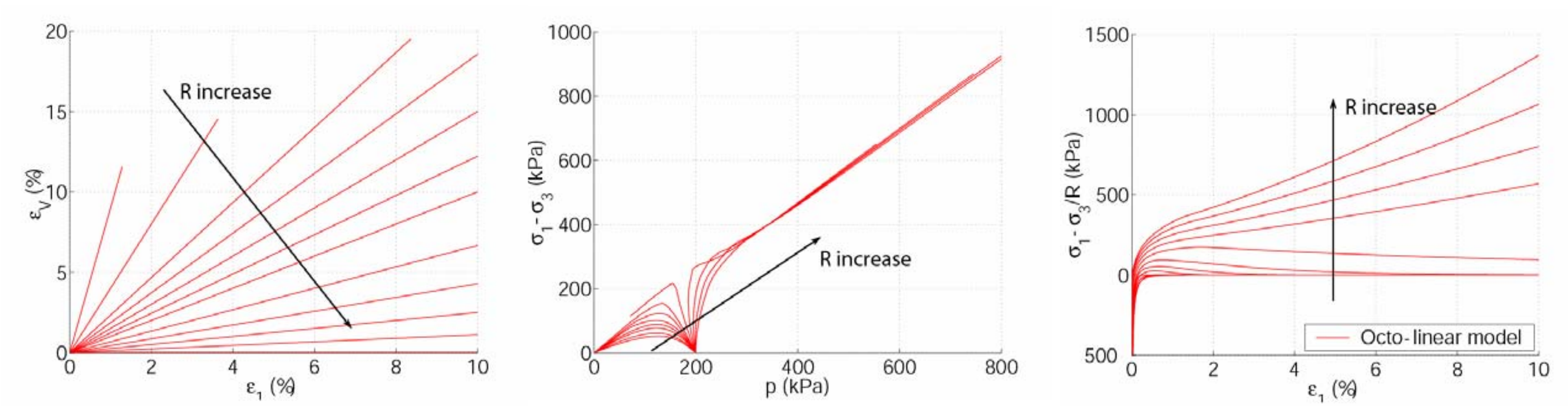

Proportional strain paths simulated by the incrementally octo-linear model for different R values (R=[0.1,0.2,0.3,0.35,0.4,0.45,0.5,0.6,0.7,0.8,0.9,1.0])

BIFURCATION DOMAIN IN AXISYMMETRY- INL2 and octolinear models, DENSE SAND

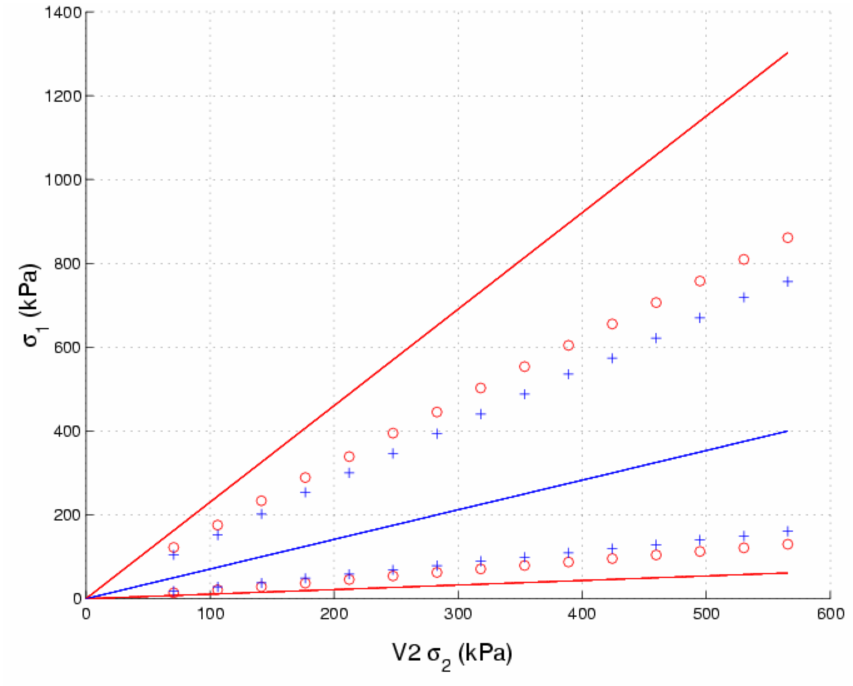

Instability domain for the dense sand in axisymmetric conditions.

σ_1- $\sqrt{2}\sigma_3$ plane in the cases of the octo-linear model (+) and the non linear one (•).

First stress directions giving a nil d^2W for the dense sand in the σ_1- $\sqrt{2}\sigma_3$ plane, with the octo-linear model (+) and the non linear one (•).

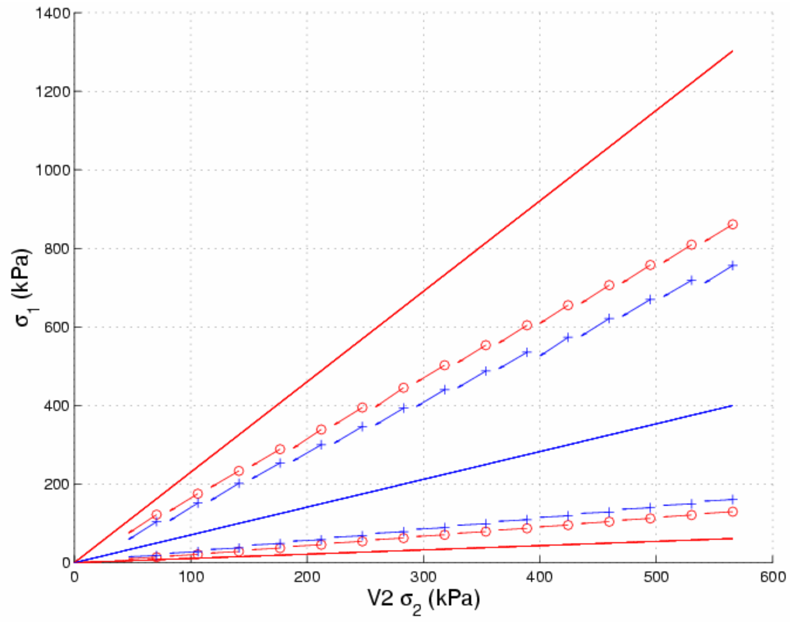

BIFURCATIONS IN AXISYMMETRIC CONDITIONS

Cones of unstable stress directions : Dense sand ; non-linear model

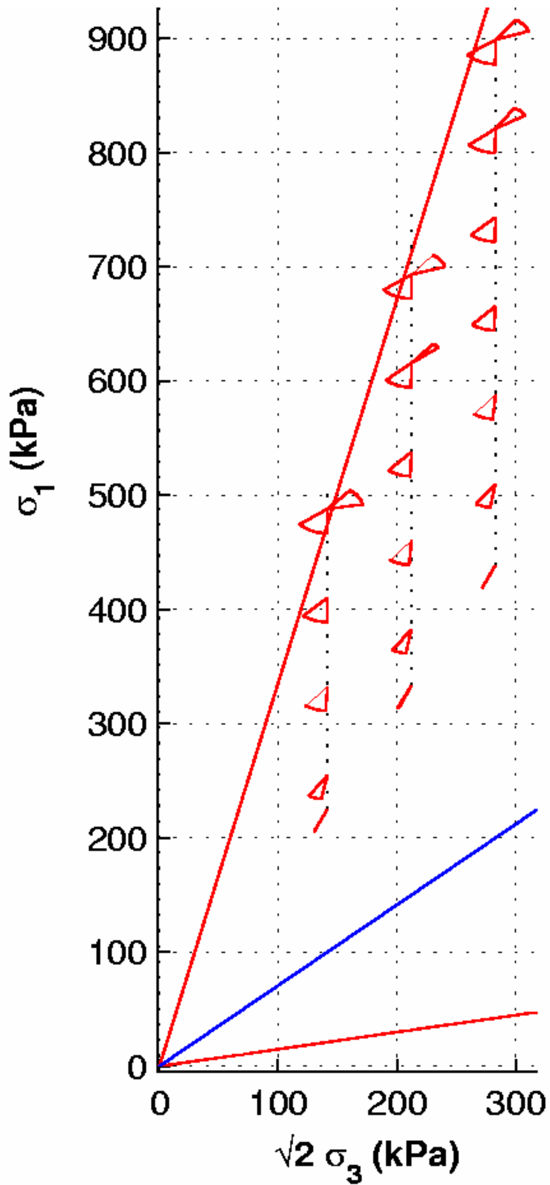

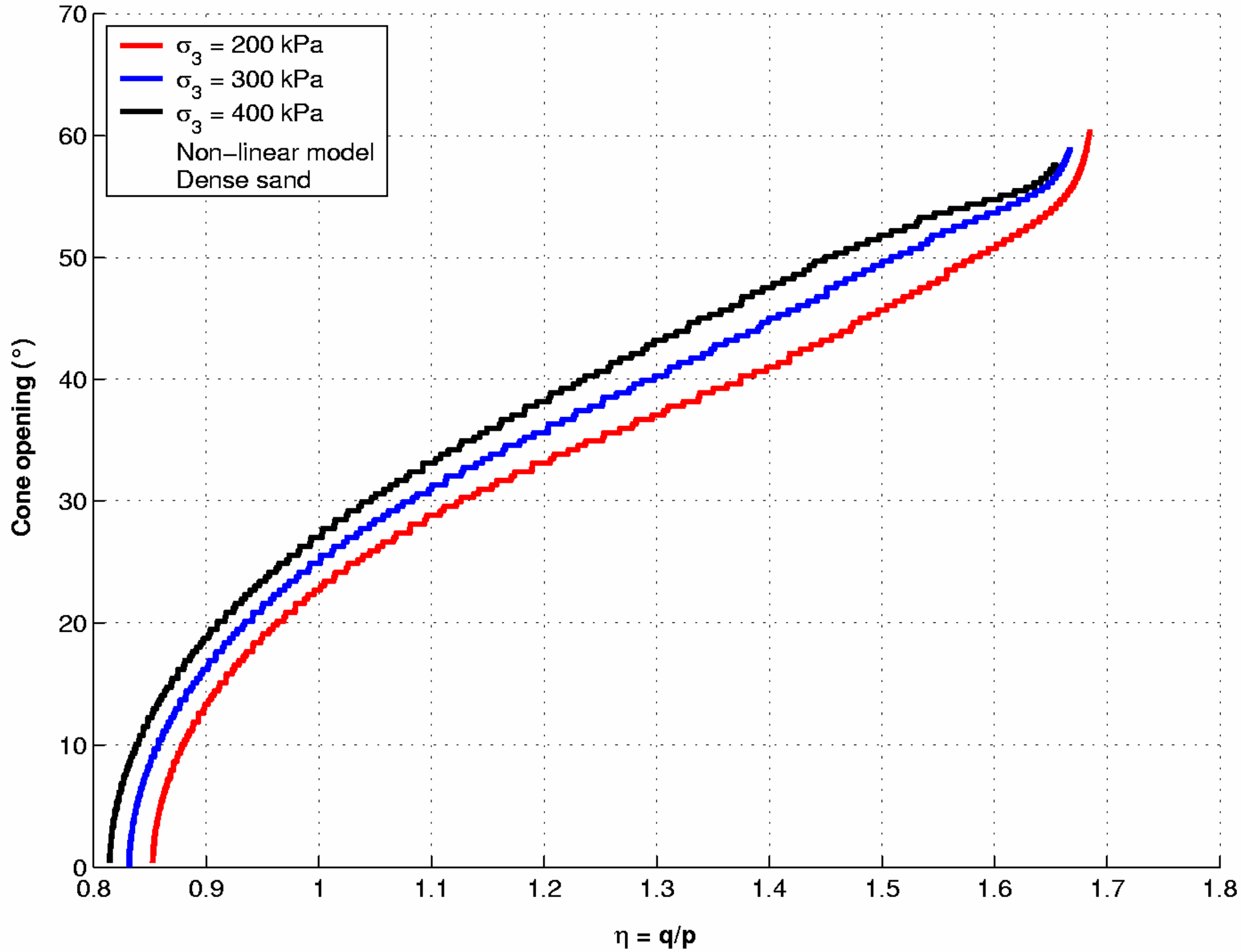

BIFURCATIONS DOMAINS IN PLANE STRAIN (H.D.V. KHOA)

octo-linear model

Bifurcation domains and first bifurcation directions corresponding to:

- **vanishing d^2W**

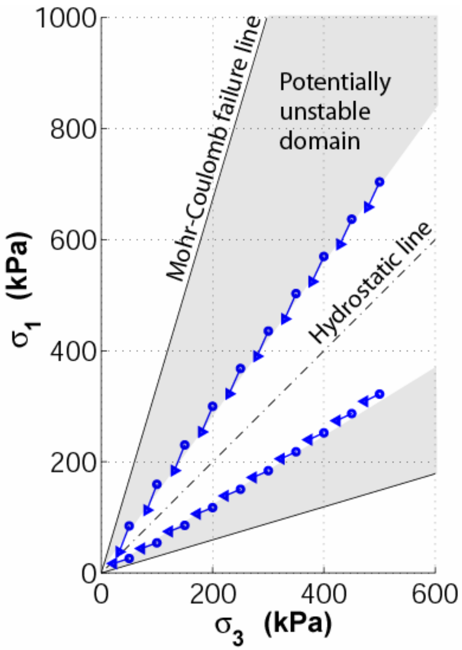

Loose Hostun sand

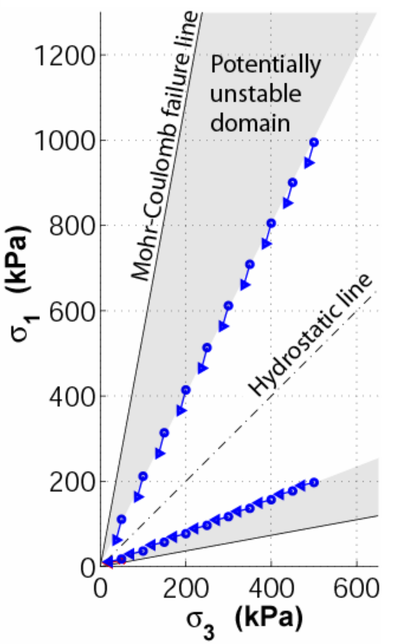

Dense Hostun sand

- **vanishing d^2W** (red) or detPs (blue)

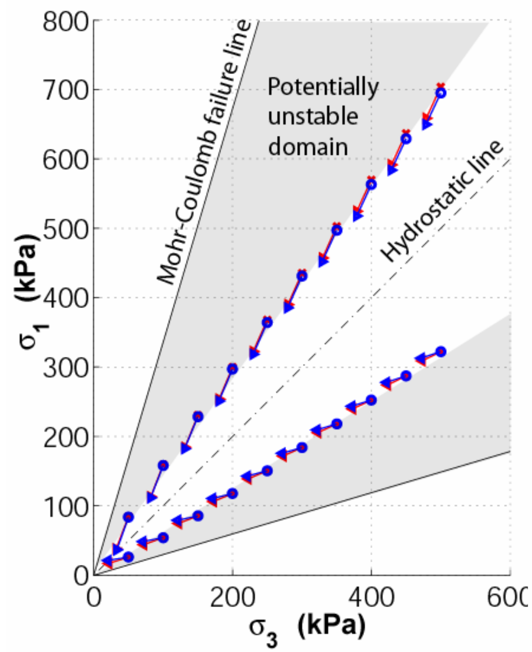

Loose Hostun sand

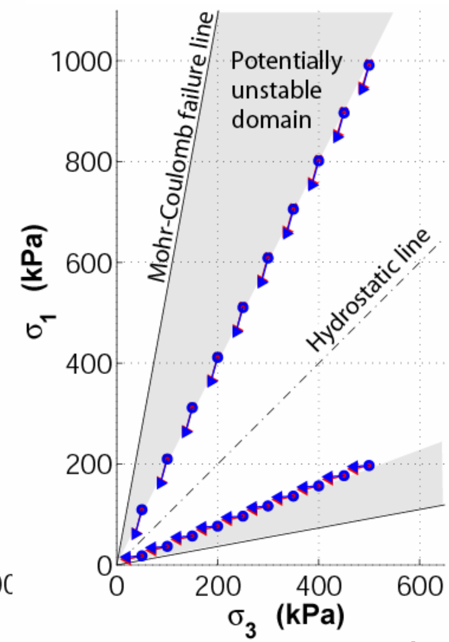

Dense Hostun sand

Bifurcation domains are **larger** for the case of loose Hostun sand than for the dense one.

The above results of two bifurcation indicators **completely numerically coincide.**

BIFURCATIONS IN PLANE STRAINS (H.D.V. KHOA)

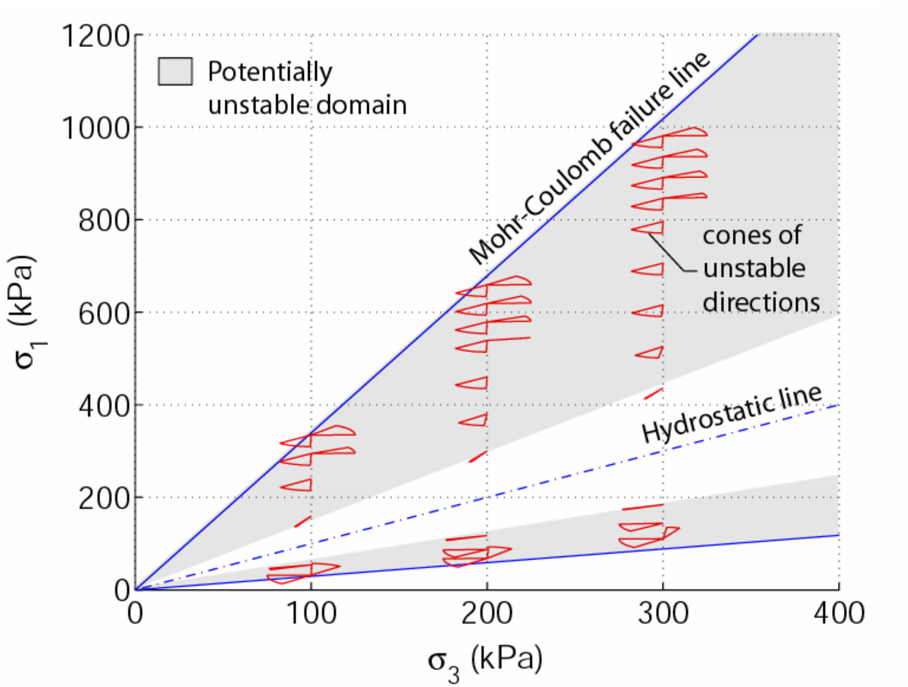

Loose Hostun sand

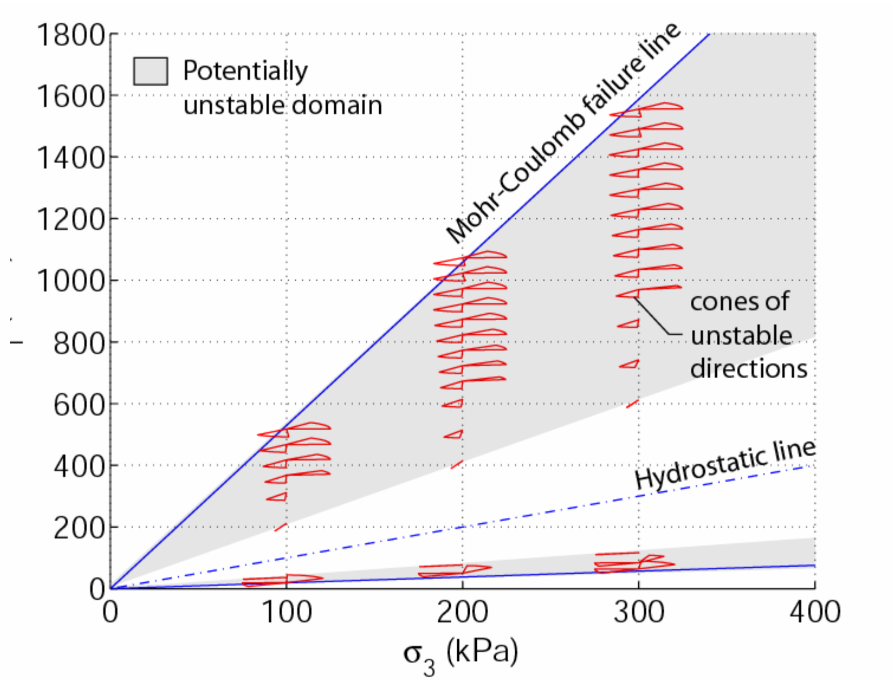

Dense Hostun sand

Boundary of the bifurcation domain and the first incremental stress directions of vanishing d^2W, according to Hill's condition, for dense Hostun sand (left) and loose Hostun sand (right). Diagrams in the (σ_1; σ_3) plane (ε_2= 0) in the case of the octo-linear constitutive model.

BIFURCATION DOMAIN (3D)

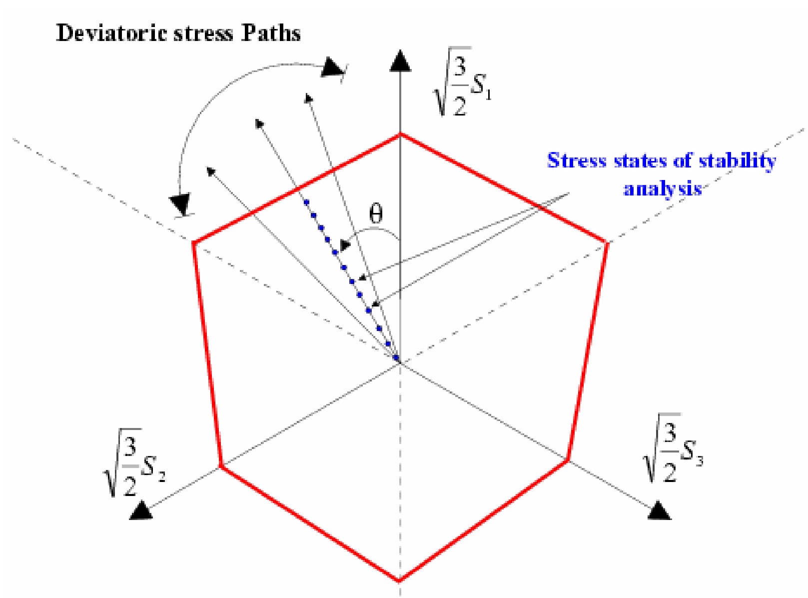

Stress paths in the deviatoric plane

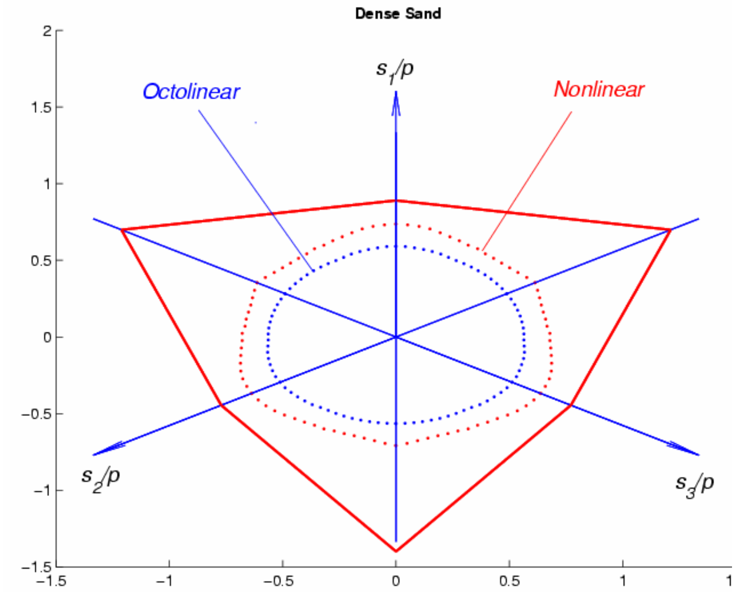

Instability surface for the dense sand (tr $\boldsymbol{\sigma}$ = 300 kPa)

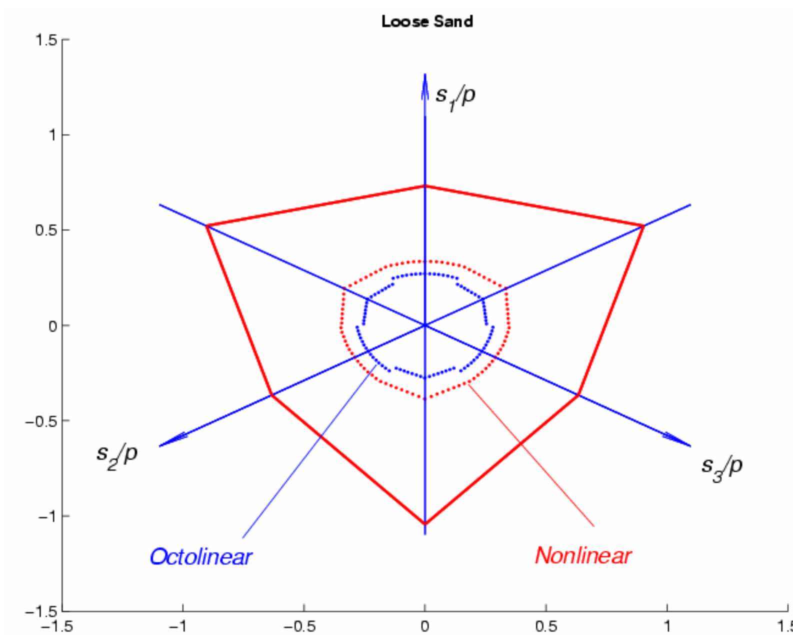

Instability surface for the loose sand (tr $\boldsymbol{\sigma}$ = 300 kPa)

THE MICRO-DIRECTIONAL MODEL (F. NICOT)

Nicot F. and Darve F. (2005) : A multiscale approach to granular materials. Mech of Mat., 37,980-1006

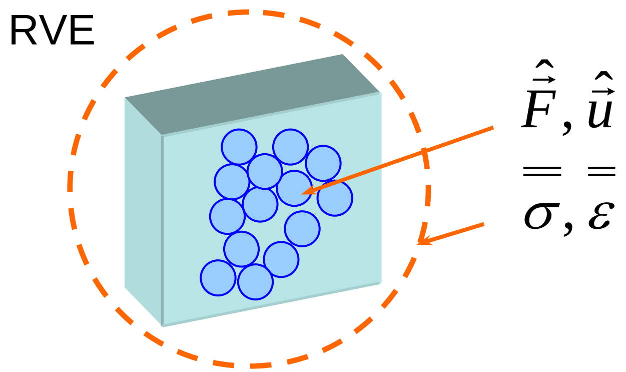

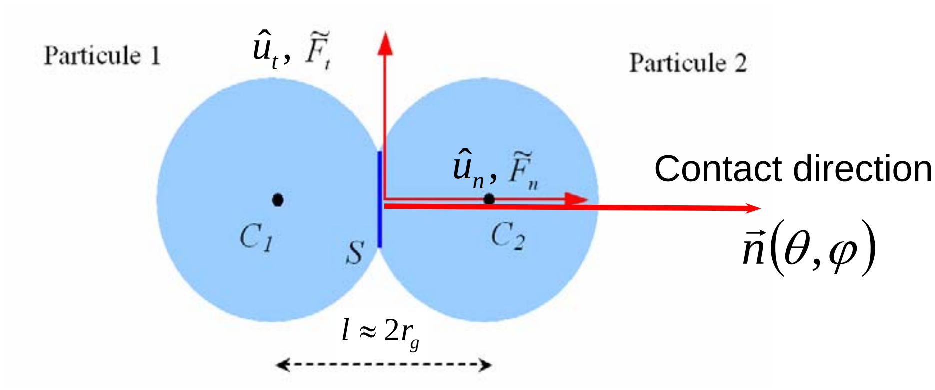

$$d\overline{\overline{\varepsilon}} \longrightarrow d\hat{\vec{u}} \longrightarrow d\hat{\vec{F}} \longrightarrow d\overline{\overline{\sigma}}$$

Strain localisation operator — **Local behaviour** — **Stress averaging**

$$d\hat{u}_i(\theta,\varphi) \approx 2r_g \, d\varepsilon_{ij} \, n_j(\theta,\varphi)$$

$$\sigma_{ij} = \frac{2r_g}{v_e} \sum_c \hat{F}_i \, n_j$$

$$d\hat{F}_n = k_n \, d\hat{u}_n$$

$$d\hat{\vec{F}}_t = \min\left\{ \left\| \hat{\vec{F}}_t + k_t \, d\hat{\vec{u}}_t \right\|, \tan\varphi_g \left(\hat{F}_n + k_n \, d\hat{u}_n \right) \right\} \frac{\hat{\vec{F}}_t + k_t \, d\hat{\vec{u}}_t}{\left\| \hat{\vec{F}}_t + k_t \, d\hat{\vec{u}}_{tt} \right\|} - \hat{\vec{F}}_t$$

(*Chang*, 1992; *Cambou*, 1993, *etc*)

Probing tests and normalised second order work

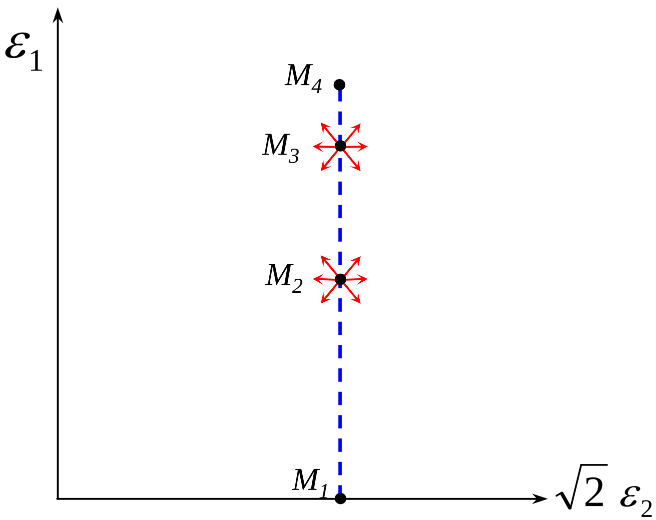

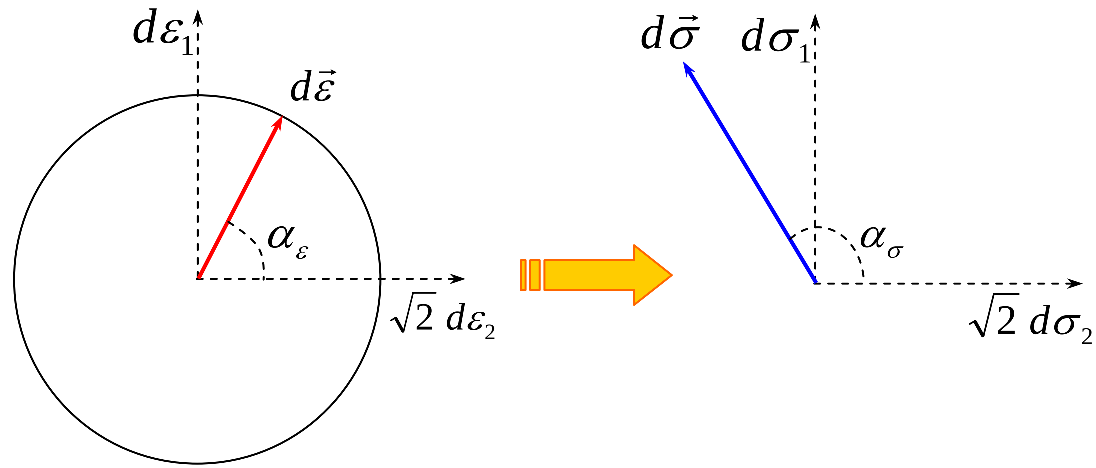

General expression of the second order work

$$d^2W = d\overline{\overline{\sigma}}\ d\overline{\overline{\varepsilon}}$$

Expression of the second order work in axisymmetric conditions

$$d^2W = d\sigma_1\ d\varepsilon_1 + 2\ d\sigma_2\ d\varepsilon_2$$

Normalised second order work

$$d^2w = \frac{d^2W}{\sqrt{d\sigma_1^{\ 2} + 2\ d\sigma_2^{\ 2}}\ \sqrt{d\varepsilon_1^{\ 2} + 2\ d\varepsilon_2^{\ 2}}}$$

Polar diagrams of the normalised second order work

Axisymmetric case

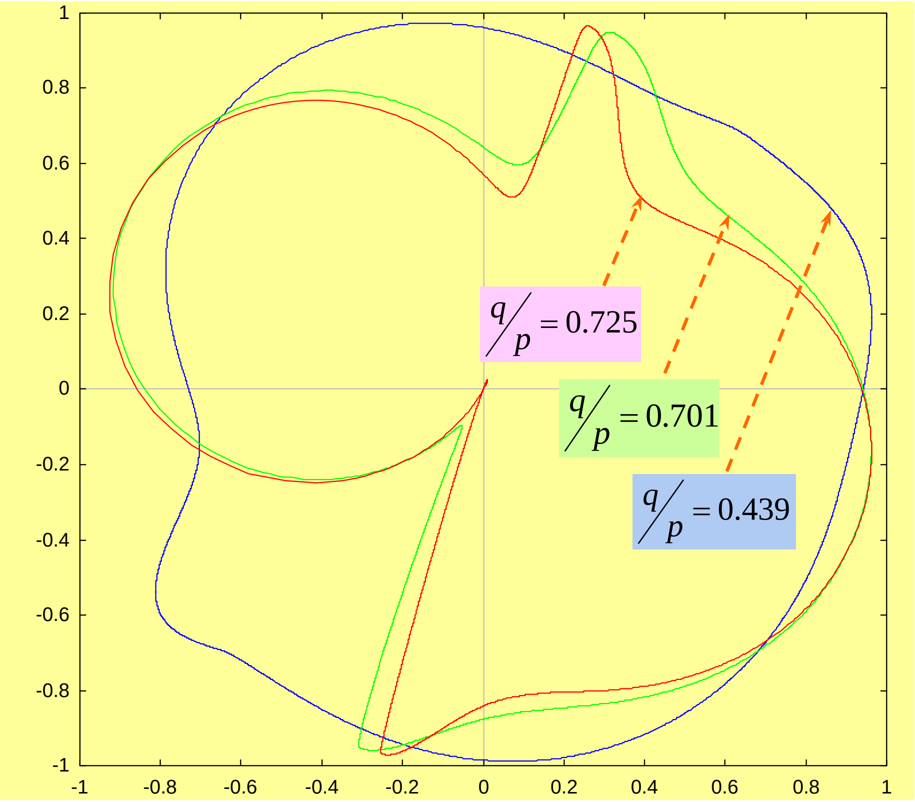

Micro-directional model

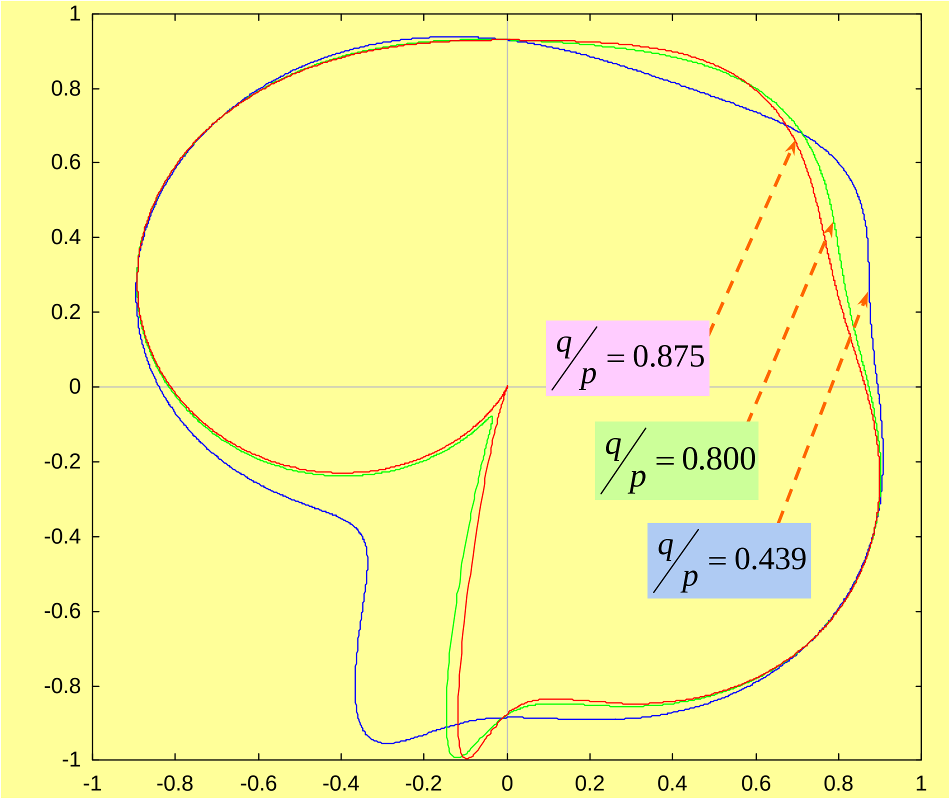

Incremental octolinear model

After Nicot, F., and Darve, F. (2005) : Micro-mechanical investigation of material instability in granular assemblies. Int. J. of Solids and Structures, 43, 3569-3595

Micro-mechanical interpretation

$$d^2W = d^2W_l + d^2W_v + d^2W_f$$

Local second order work

Change in volume

Change in fabric

$$d^2W_l = \frac{3}{2\pi\, N_g\, r_g^{\ 2}} \frac{\rho_o}{\rho_g} \iint_{[o;\pi]^2} \frac{d\hat{F}_i(\theta,\varphi)\, d\hat{u}_i(\theta,\varphi)\, \omega_e(\theta,\varphi)}{1-\varepsilon_{kk}} \sin\varphi\, d\theta\, d\varphi$$

$$d^2W_f = \frac{3}{2\pi\, N_g\, r_g^{\ 2}} \frac{\rho_o}{\rho_g} \iint_{[o;\pi]^2} \frac{\hat{F}_i(\theta,\varphi)\, d\hat{u}_i(\theta,\varphi)\, d\omega_e(\theta,\varphi)}{1-\varepsilon_{kk}} \sin\varphi\, d\theta\, d\varphi$$

$$d^2W_v = \frac{3}{2\pi\, N_g\, r_g^{\ 2}} \frac{\rho_o}{\rho_g} \iint_{[o;\pi]^2} \frac{\hat{F}_i(\theta,\varphi)\, d\hat{u}_i(\theta,\varphi)\, \omega_e(\theta,\varphi)\, d\varepsilon_{kk}}{(1-\varepsilon_{kk})^2} \sin\varphi\, d\theta\, d\varphi$$

Micro-mechanical interpretation

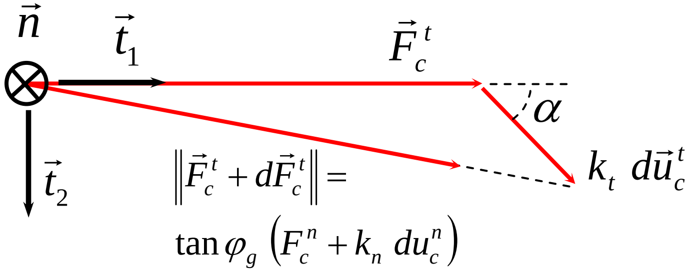

Plastic case

Quadratic form
of the second order work

$$d^2\hat{W} = d\hat{\vec{F}} \cdot d\hat{\vec{u}} = d\hat{F}_n\ d\hat{u}_n + d\hat{F}_{t_1}\ d\hat{u}_{t_1} + d\hat{F}_{t_2}\ d\hat{u}_{t_2}$$

In the plastic case

$$d^2\hat{W} = k_n\ d\hat{u}_n^{\ 2} + \tan\varphi_g\ \cos\alpha\ k_n\ d\hat{u}_n\ d\hat{u}_t + k_t\ \sin^2\alpha\ d\hat{u}_t^{\ 2}$$

$$d^2\hat{W} \le 0 \iff \left\{ \begin{array}{l} d\hat{u}_n \le 0 \\ \tan\alpha \le \dfrac{\tan\varphi_g}{2}\sqrt{\dfrac{k_n}{k_t}} \qquad \alpha \in \left[-\dfrac{\pi}{2} ; \dfrac{\pi}{2} \right] \\ d\hat{u}_t \in \left[U_1 ; U_2 \right] \end{array} \right.$$

$$U_i = \frac{-\tan\varphi_g\ k_n\ d\hat{u}_n\ \cos\alpha \left(1 + \xi_i \sqrt{1 - 4\,\dfrac{k_t\ \tan^2\alpha}{k_n\ \tan^2\varphi_g}} \right)}{2\ k_t\ \sin^2\alpha}$$

$$\xi_1 = -1 \qquad \xi_2 = 1$$

Discrete analysis of stability from D.E.M. computations (L. Sibille)

The Discrete Element Model :

- SDEC software (*Donzé & Magnier 1997*): molecular dynamics approach such as *Cundall*'s one (*1979*).

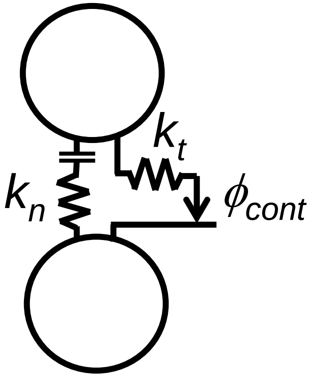

- Contact interaction defined by 3 mechanical parameters:

$$10^5 \leq k_n \leq 10^6\, N/m$$

$$k_t = k_n / 0.42$$

$$\Phi_{cont} = 35°$$

- Cubic form of the specimen; 10 000 spheres; continuous size distribution; dense specimen:

$$2 \leq D_{sphere} \leq 9\, mm$$

For p = 100 kPa: $n = 0.38$

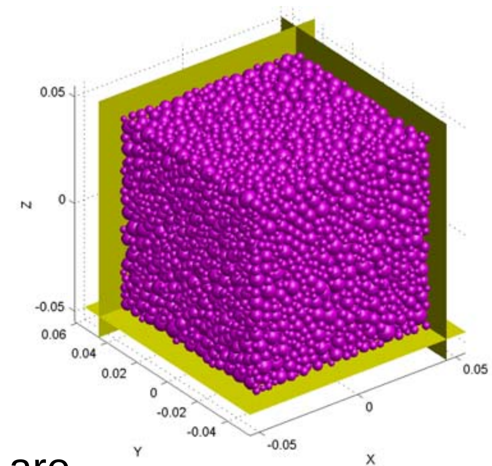

- All paths in principal stress (σ_1, σ_2, σ_3) or strain (ε_1, ε_2, ε_3) spaces are allowed. In this lecture: axi-symmetric conditions only.

Discrete analysis of stability from D.E.M. computations (L. SIBILLE)

Stress probes :

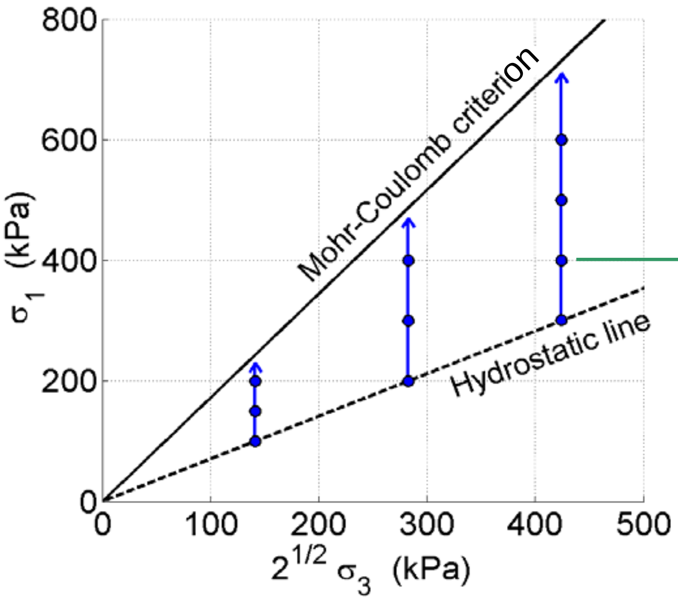

The initial axi-symmetric stress states:

1. isotropic compression (100, 200 or 300 kPa),
2. triaxial drained compression ($\sigma_2 = \sigma_3 = cst.$) characterised by:

$$\frac{q}{p} = \frac{\sigma_1 - \sigma_3}{(\sigma_1 + \sigma_2 + \sigma_3)/3}$$

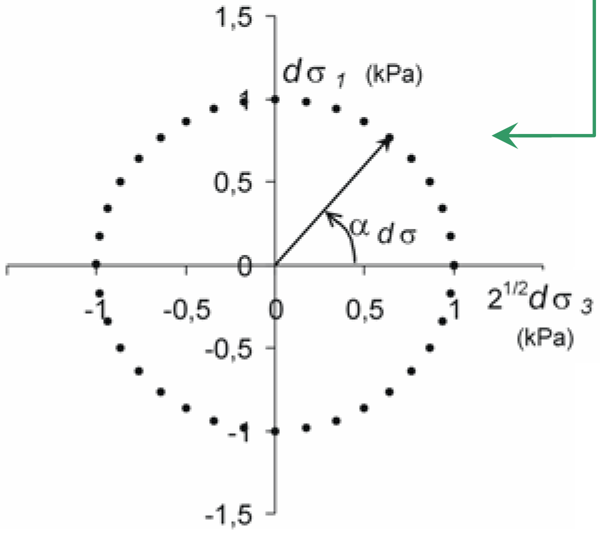

The loading program:

- defined in the Rendulic plane of stress increments,
- $\left| d\sigma \right| = \sqrt{\left(d\sigma_1 \right)^2 + \left(\sqrt{2}\, d\sigma_3 \right)^2} = cte = 1kPa$
- $0 \leq \alpha_{d\sigma} < 360°$

$\rightarrow$ response vectors $d\varepsilon$ defined in dual plane ($\sqrt{2}d\varepsilon_3, d\varepsilon_1$).

$\rightarrow$ $d^2W = d^2W(\alpha_{d\sigma})$

Unstable directions :

Diagram of $f(\alpha_{d\sigma}) = d^2W_{norm.} + c$ with: $\begin{cases} d^2W_{norm.} = \dfrac{d\sigma \cdot d\varepsilon}{|d\sigma||d\varepsilon|} \\ c \text{ such as: } f(\alpha_{d\sigma}) > 0 \end{cases}$

σ_3 = 100 kPa

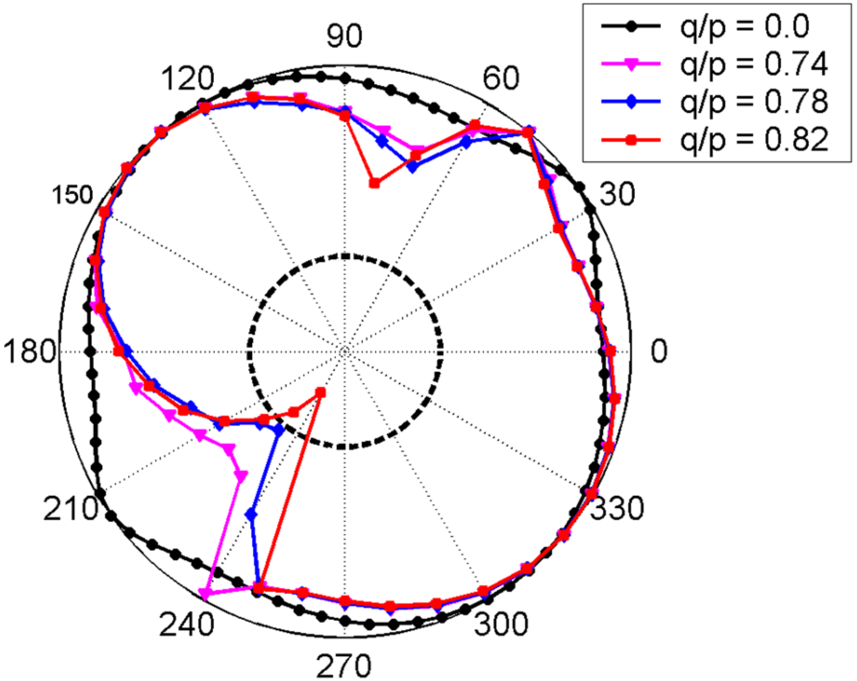

σ_3 = 200 kPa

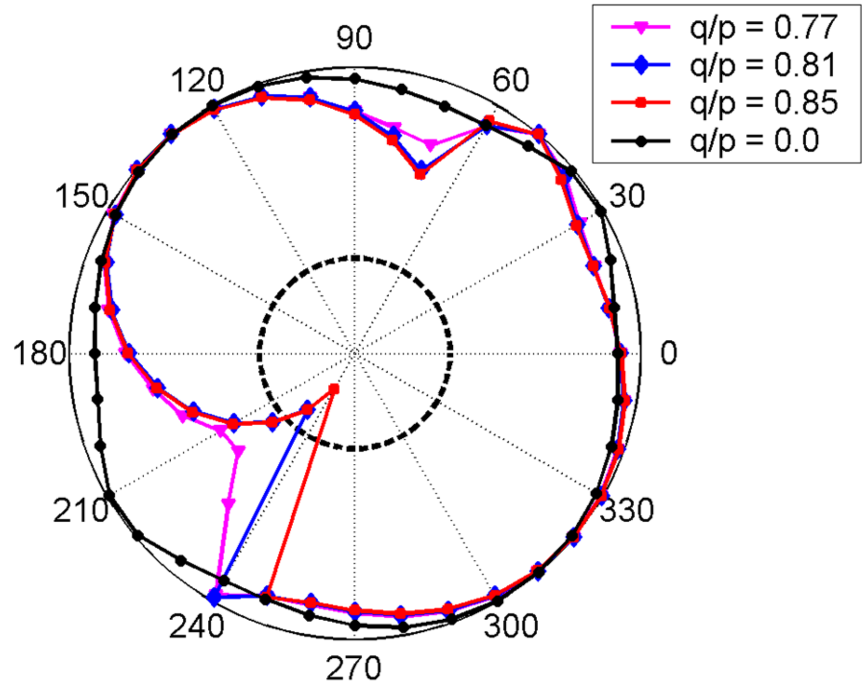

→ Cones of "unstable" stress directions observed with the D.E.M.

Discrete analysis of stability from D.E.M. computations

Cones of unstable stress directions : D.E.M. and Incremental Non-Linear model

Discrete Element Model

- *d²W* > 0
- Cones of unstable directions (L. Sibille)

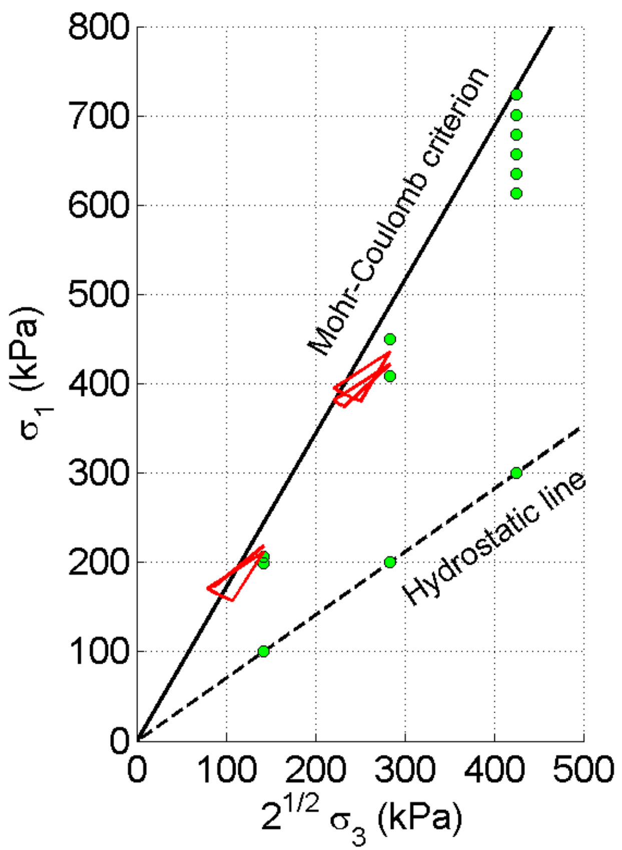

Macroscopic phenomenological relation *(I.N.L.2 model)*

calibrated on the drained triaxial responses of D.E.M. (L.*Scholtes*).

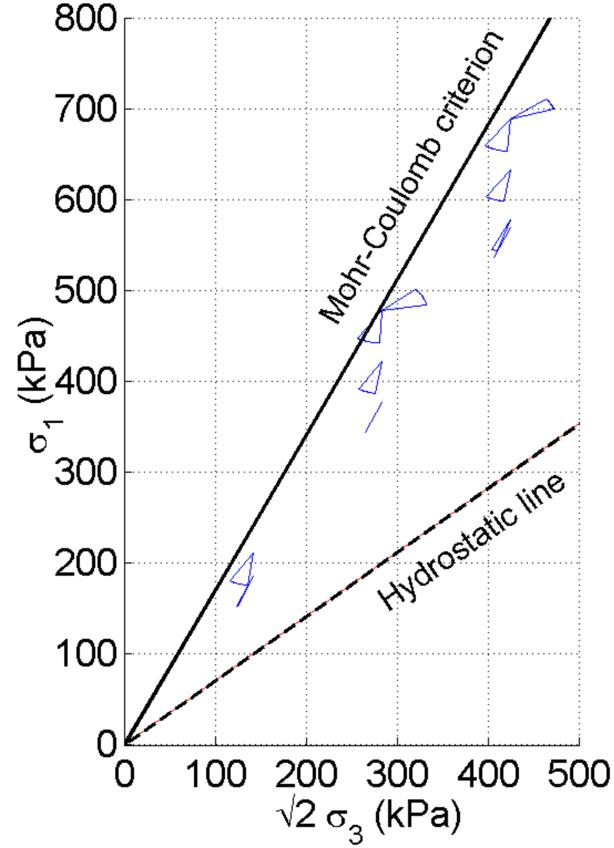

2^{nd} step – from the bifurcation point to the failure

- *Imposimato and Nova (1998)* **shown that the full controllability of a loading programme defined by its control parameters can be lost before reaching the plastic limit condition.**
- **The control parameters can be linear combinations of stresses or strains (e.g. volumetric strains).**

Loose specimen, $\eta = 0.46$, $\alpha = 215.3$ deg ($q = cst$)

- Stress probe is fully stress controlled $\rightarrow$ no failure observed.
- Can we choose others control parameters ?

$$d^2W = d\sigma_1\, d\varepsilon_1 + 2\, d\sigma_3\, d\varepsilon_3 = dq\, d\varepsilon_1 + d\sigma_3\, d\varepsilon_v$$

- Can we control the loading programme defined by:

$$dq = 0 \text{ and } d\varepsilon_v = -\,0.002\ \% \text{ (dilatancy) ?}$$

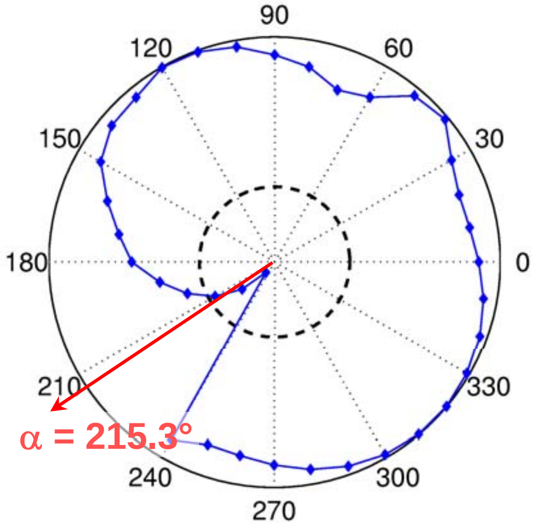

$$f(\alpha) = d^2W_{norm.} + c$$

Comparison of the response of the numerical specimen controlled by:

d*q* = 0 and dσ_3 < 0

or by d*q* = 0 and dε_v < 0

⇒ Loss of controllability for d*q* = 0 and dε_v < 0, the specimen totally collapses.

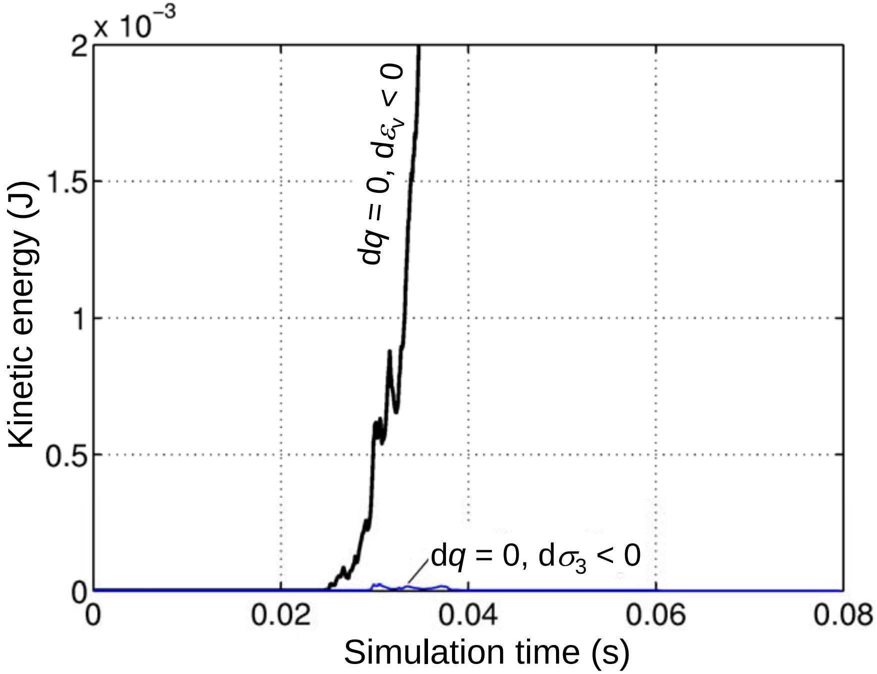

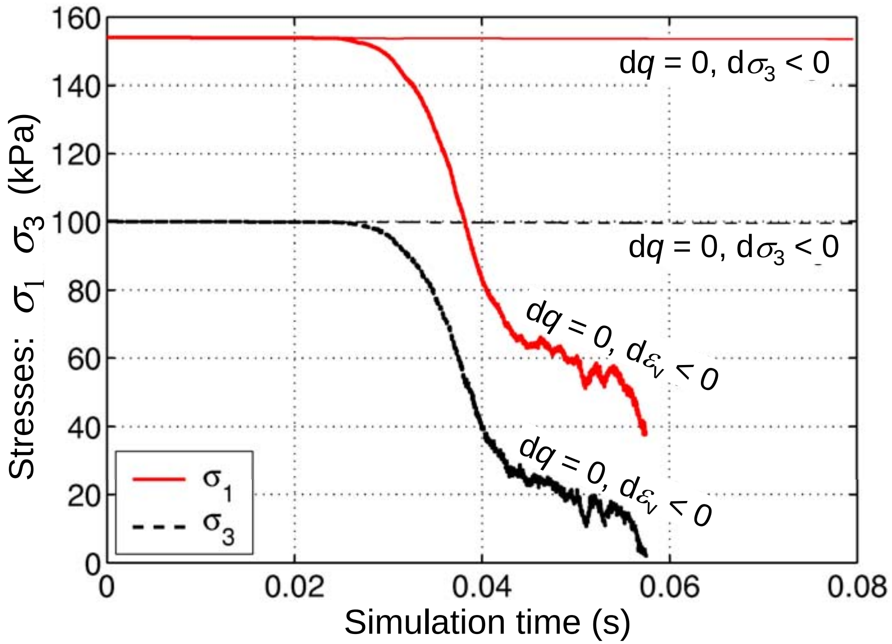

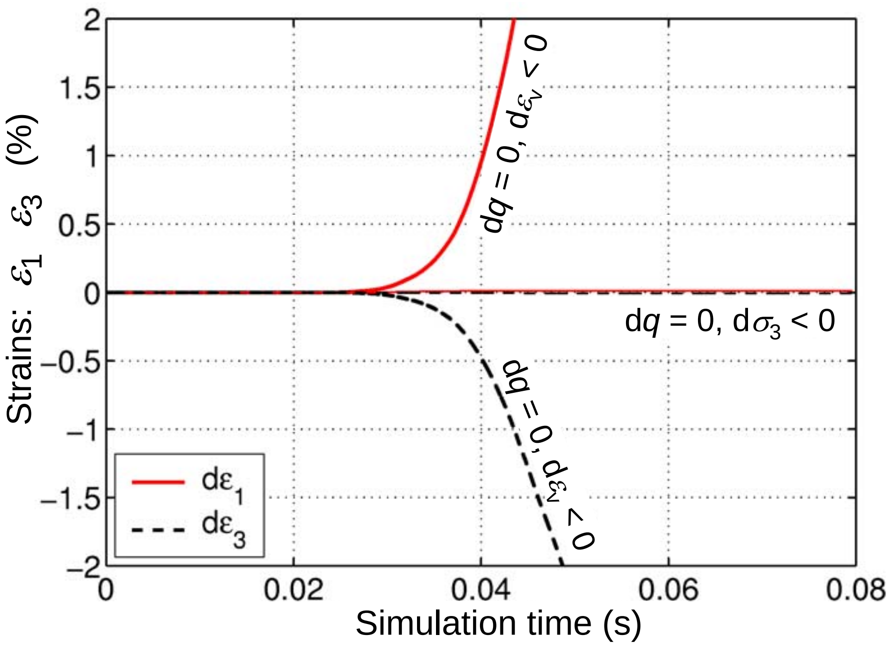

2^{nd} step – from the bifurcation point to the failure

Generalization to proportional stress paths

$$d^2W = d\sigma_1\, d\varepsilon_1 + 2\, d\sigma_3 d\varepsilon_3$$

$$d^2W = d\varepsilon_1 \left(d\sigma_1 - \frac{d\sigma_3}{R} \right) + \frac{d\sigma_3}{R} \left(d\varepsilon_1 + 2R\, d\varepsilon_3 \right)$$

with $R = cst.$ for a given loading path.

Can we control the loading programme defined by:

$d\sigma_1 - d\sigma_3 / R = 0$ and $d\varepsilon_1 + 2R\, d\varepsilon_3 = -0.002\ \%$?

with: $R = 1.94$ ($\alpha = 200°$, $d^2W > 0$)
$R = 1.22$ ($\alpha = 210°$, $d^2W < 0$)
$R = 1.00$ ($\alpha = 215.3°$, $d^2W < 0$)
$R = 0.843$ ($\alpha = 220°$, $d^2W < 0$)
$R = 0.593$ ($\alpha = 230°$, $d^2W < 0$)
$R = 0.408$ ($\alpha = 240°$, $d^2W > 0$)

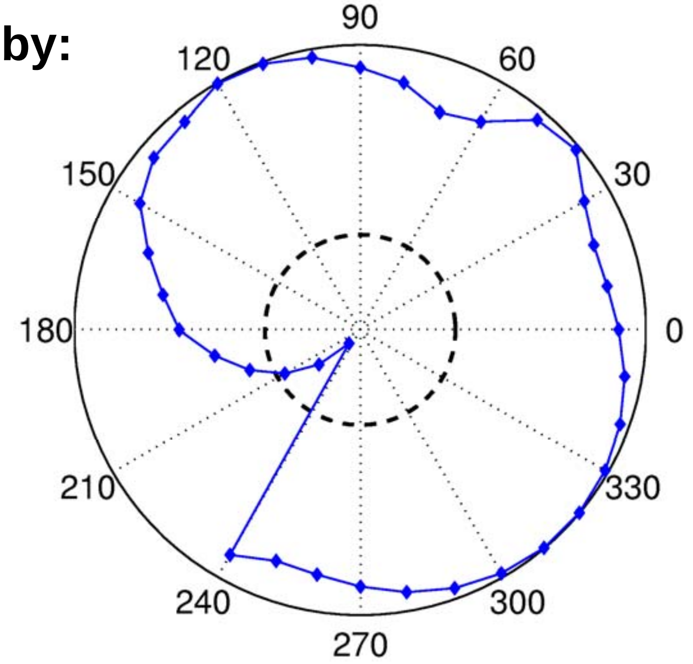

$$f(\alpha) = d^2W_{norm.} + c$$

2^{nd} step – from the bifurcation point to the failure

- The loading programme is controllable for *R* = 1.94 and 0.408 ($d^2W > 0$).
- Loss of controllability for *R* = 1.00; 0.843; 0.593 ($d^2W < 0$).
- For *R* = 1.22 ($d^2W < 0$ but stress direction close to the border of the cone) the loss of controllability is not total.

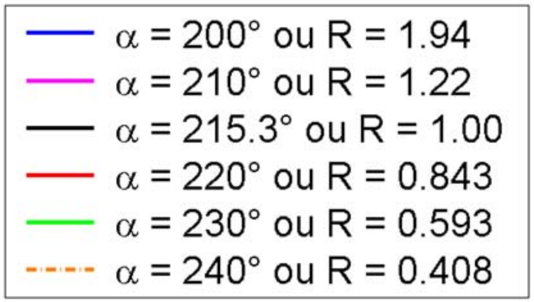

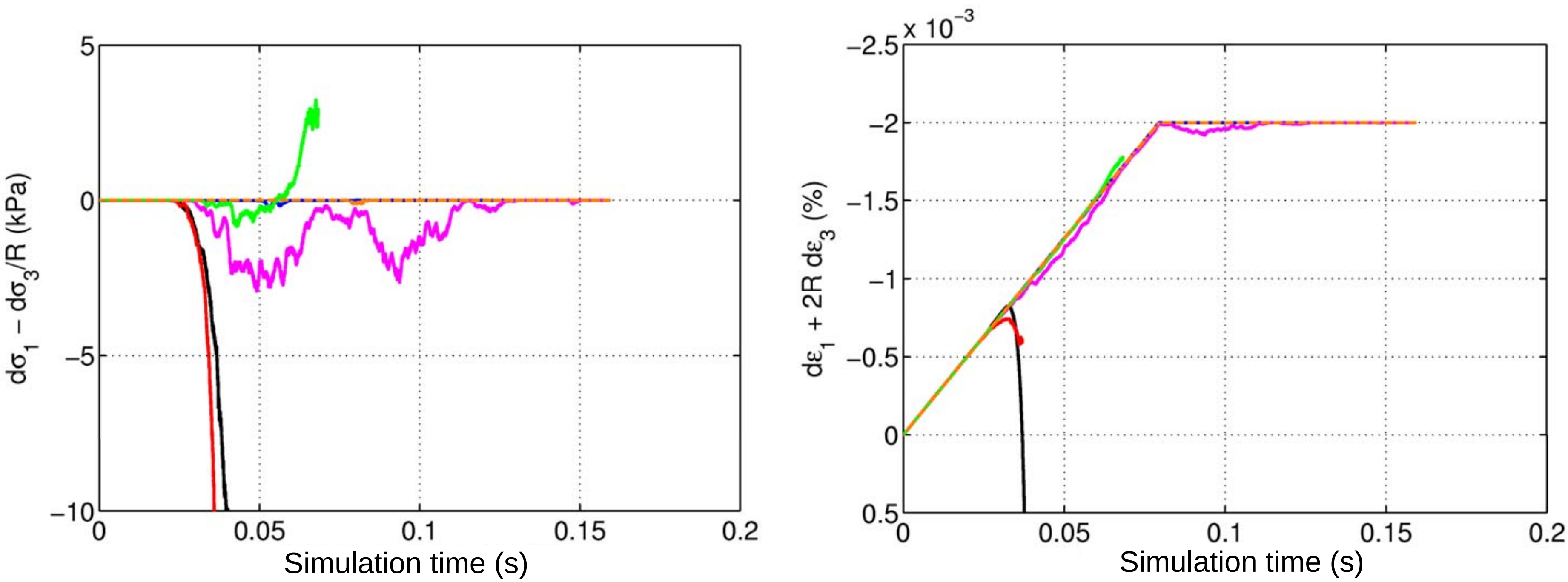

2^{nd} step – from the bifurcation point to the failure

- For R = 1.94 and 0.408 ($d^2W > 0$) a new stable state close to the initial one is reached.
- Total collapse for R = 1.00; 0.843; 0.593 ($d^2W < 0$).
- For R = 1.22 ($d^2W < 0$ but stress direction close to the border of the cone) the collapse is partial.

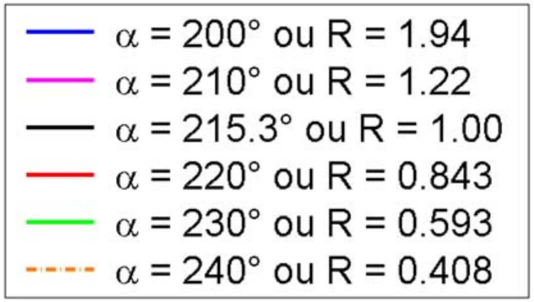

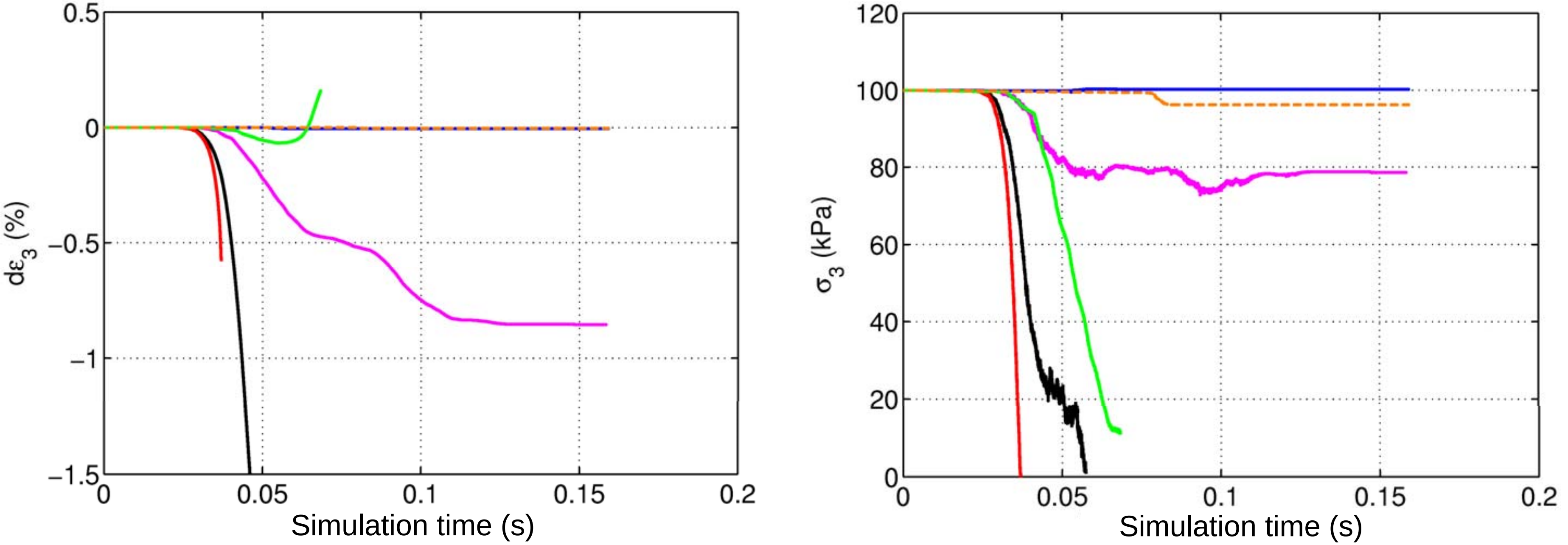

⇒ Loading parameters exist such as the specimen collapses from a bifurcation point detected by the sign of d^2W.

2^{nd} step – from the bifurcation point to the failure

In their tests *Chu et al. 2003* **do not apply any loading path. They verify if a mechanical state governed by specific control parameters can be sustained** (*Notion of loss of sustainability, Nicot and Darve 2006).*

- **Control of the mechanical state by:**

  $d\sigma_1 - d\sigma_3 / R = 0$ and $d\varepsilon_1 + 2R\, d\varepsilon_3 = 0$

  with: $R = 4.01$ ($\alpha = 190°$, $d^2W > 0$)
  $R = 1.94$ ($\alpha = 200°$, $d^2W > 0$)
  $R = 1.22$ ($\alpha = 210°$, $d^2W < 0$)
  $R = 1.00$ ($\alpha = 215.3°$, $d^2W < 0$)
  $R = 0.843$ ($\alpha = 220°$, $d^2W < 0$)
  $R = 0.593$ ($\alpha = 230°$, $d^2W < 0$)
  $R = 0.408$ ($\alpha = 240°$, $d^2W > 0$)
  $R = 0.257$ ($\alpha = 250°$, $d^2W > 0$)

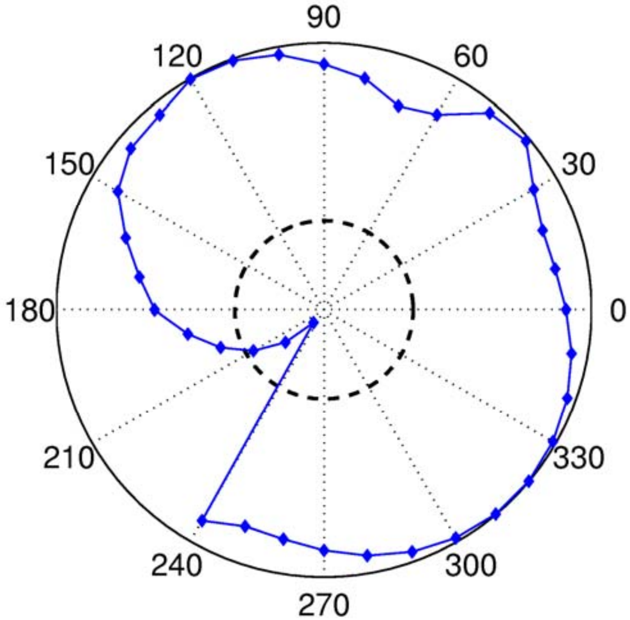

$$f(\alpha) = d^2W_{norm.} + c$$

- **Small perturbation of the numerical specimen**

  External input of kinetic energy ($1\ 10^{-5}$ J) to the specimen by excitements of some floating grains (simulation without gravity).

2nd step – from the bifurcation point to the failure

- For *R* = 4.01; 1.94; 0.408; 0.257 ($d^2W > 0$) a new stable state is reached.
- Total collapse for *R* = 1.00; 0.843; 0.593 ($d^2W < 0$).
- For *R* = 1.22 ($d^2W < 0$ but stress direction close to the border of the cone) the collapse is partial.

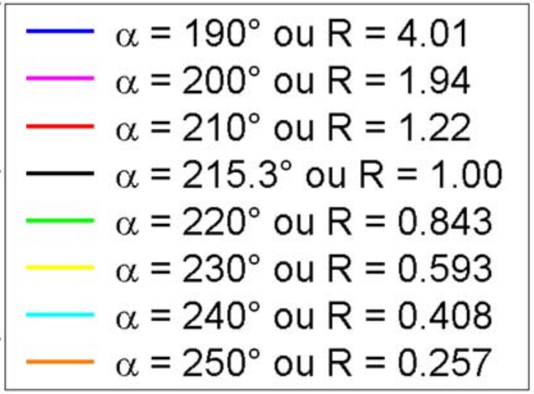

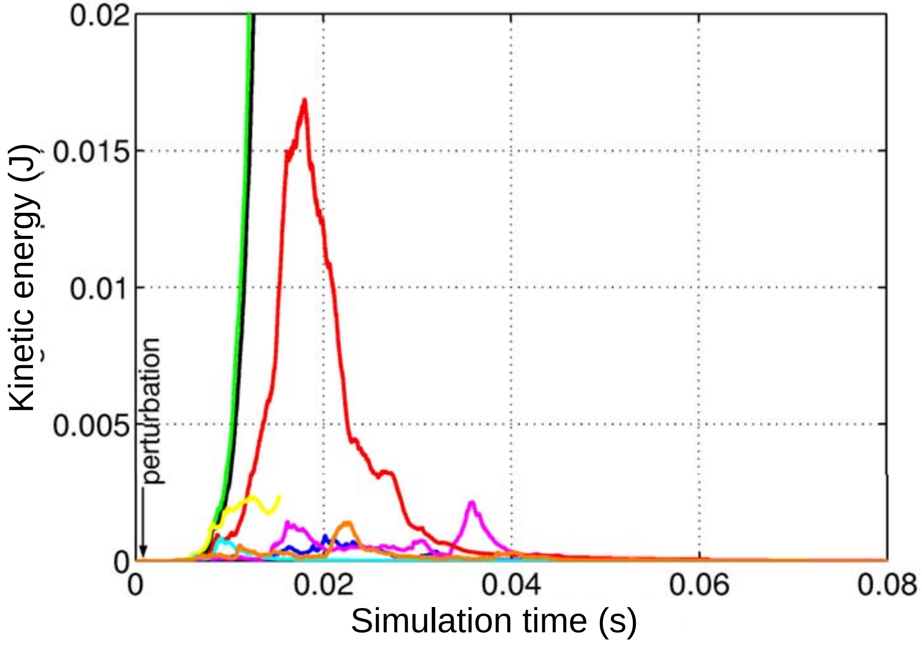

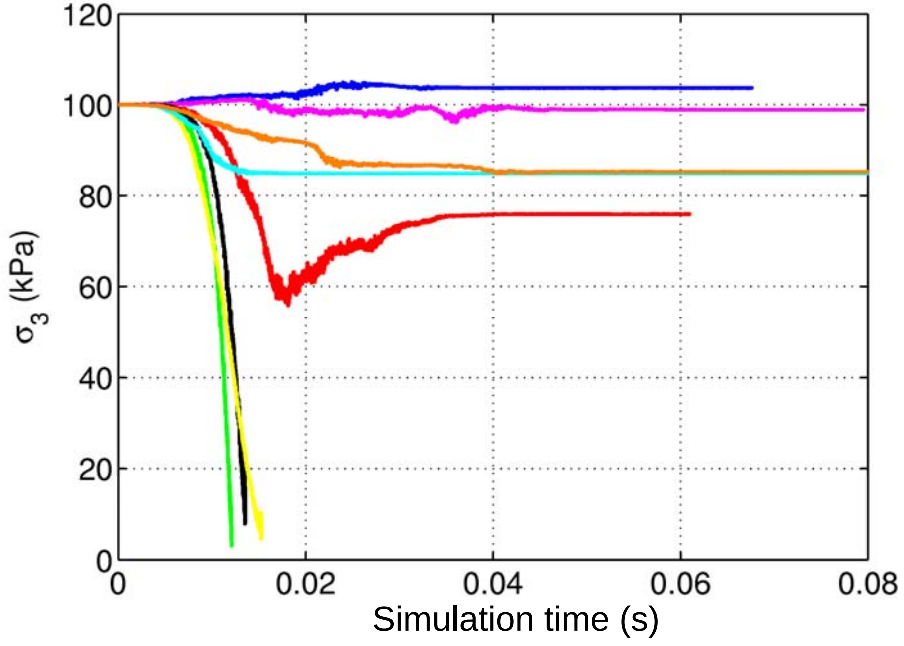

CONCLUSIONS

1. Phenomenological analysis : for non associated materials like geomaterials, there is not a single plastic limit surface where failure occurs, but rather a whole domain in the stress space where bifurcations, losses of uniqueness, instabilities … i.e. FAILURES can appear, according to :

   - the stress-strain history
   - the current direction of loading
   - the loading mode

   In this bifurcation domain, various failure modes can develop (material instabilities leading to diffuse or localized failures, geometric instabilities, …)

   Second order work criterion seems to detect diffuse failure

2. Micromechanical analysis : it confirms these analyses. Moreover a new micro-mechanical understanding of these material instabilities is proposed by considering the local, discrete, second order work at the grain level.

3. Discrete element analysis : bifurcation domains and cones of unstable stress-strain directions also exhibited in good qualitative agreement. Diffuse failure was simulated exactly for the conditions predicted by the theory.

These 3, basically different, methods give similar results

Some recent contributions

Book : Degradations and Instabilities in Geomaterials, F. Darve and I. Vardoulakis eds, Springer publ., 367 pages, 2005

Papers :

- Darve, F., Servant G., Laouafa F., Khoa H.D.V. (2004): Failure in geomaterials, continuous and discrete analyses, Comp. Meth. In Applied Mech. and Eng., vol. 193, 27-29, 3057-3085.
- Nicot, F., and Darve, F. (2005) : A multiscale approach to granular materials. Mechanics of Materials, 37, 980-1006
- Darve, F., and Nicot, F. (2005): On incremental non linearity in granular media, phenomenological and multi-scale views.(I) Int. J. Numerical Analytical Methods in Geomech., vol.29, n°14, 1387-1410
- Darve, F., and Nicot, F. (2005): On flow rule in granular media, phenomenological and multi-scale views (II). Int. J. Numerical Analytical Methods in Geomech. ,vol. 29, n°14, 1411-1432
- Nicot, F., and Darve, F. (2005) : Micro-mechanical investigation of material instability in granular assemblies. Int. J. of Solids and Structures, 43, 3569-3595
- H.D.V. Khoa, I.O. Georgopoulos, F. Darve, F. Laouafa (2006): Diffuse failure in geomaterials , experiments and modelling, Comp. Geotechn., vol.33, n°1, 1-14.
- Nicot, F., and Darve, F. (2006) : On the elastic and plastic strain decomposition in granular materials., Granular Matter, vol.8, n°3, 221-237
- Sibille L., Nicot F., Donze F.V., Darve F. (2007) : Material instability in granular assemblies from fundamentally different models, Int. J. Num. Anal. Methods in Geomechanics, vol. 31, n°3, 457-482
- Nicot F., Sibille L., Donze F., Darve F. (2007) : From microscopic to macroscopic second-order work in granular assemblies, Mechanics of Materials, vol.39, n°7, 664-684

II Landslides modelling : Trévoux and Petacciato examples

FINITE ELEMENT MODELLING OF THE TREVOUX AND PETACCIATO LANDSLIDES BY TAKING INTO ACCOUNT UNSATURATED HYDRO-MECHANICAL COUPLING

Application to Trévoux and Petacciato landslides

Trévoux

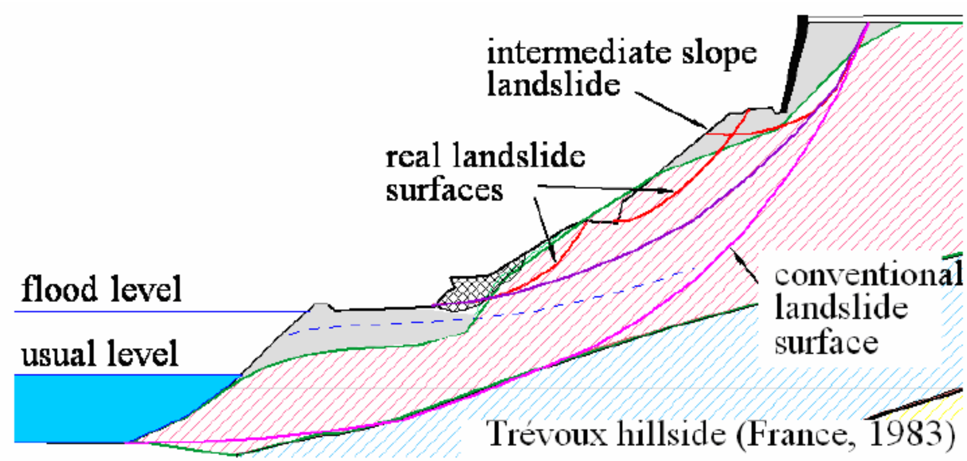

Petacciato

deep crack (square in front of the parish church).

“Vaccareggia”, crack on the road near the slide boundary.

The Trevoux site

Geographic location of the studied area

The Trevoux site

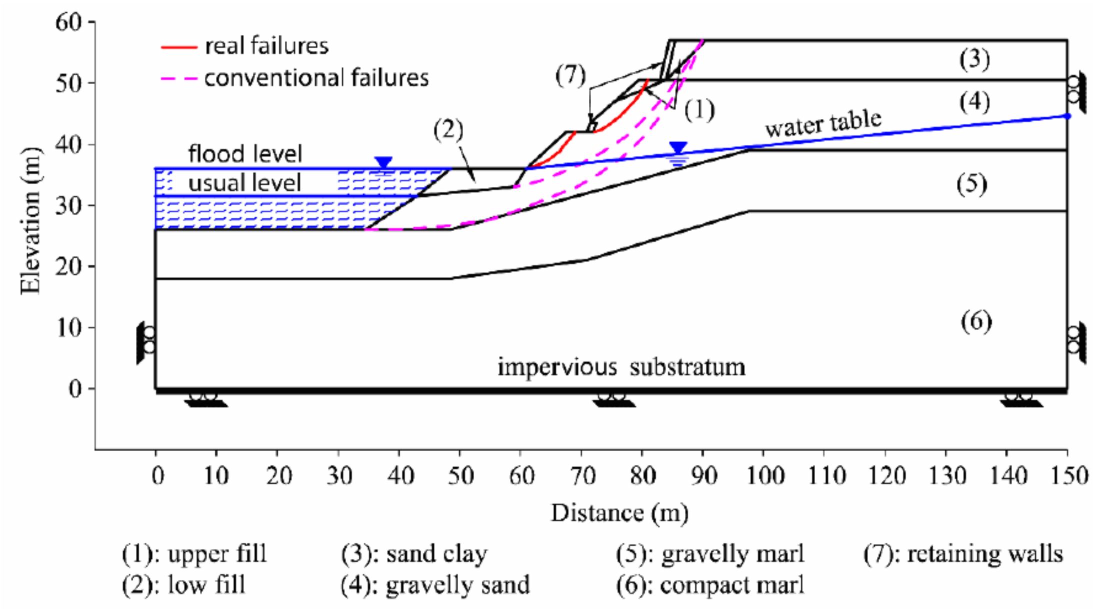

Typical cross section of the Trevoux landslide

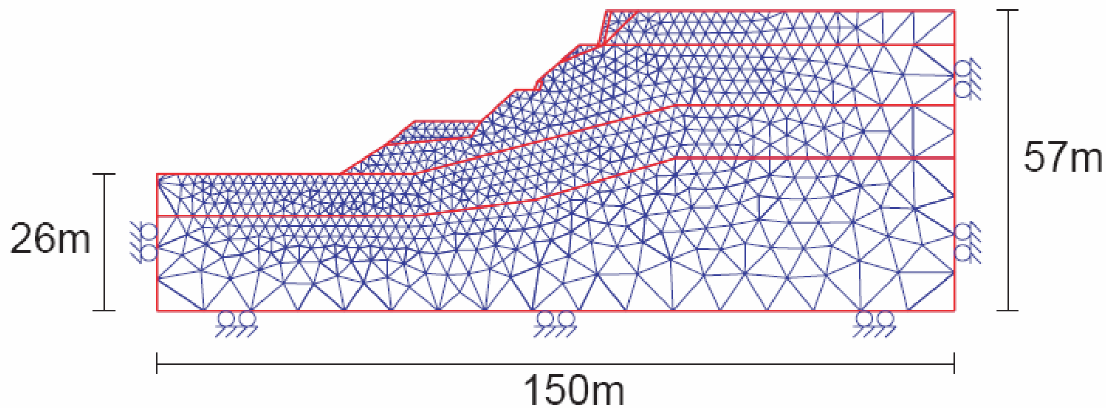

Finite element mesh of the Trevoux landslide

The Petacciato site

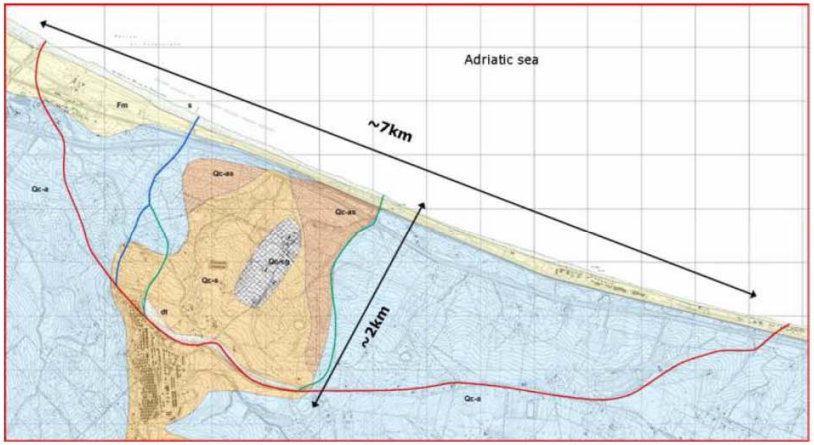

Geographic location of the studied area

The Petacciato site

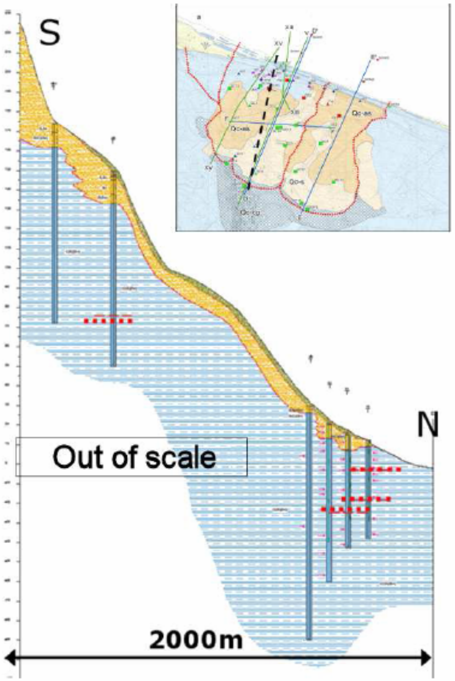

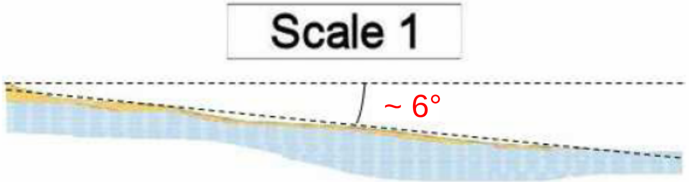

Typical cross-section of the Petacciato landslide

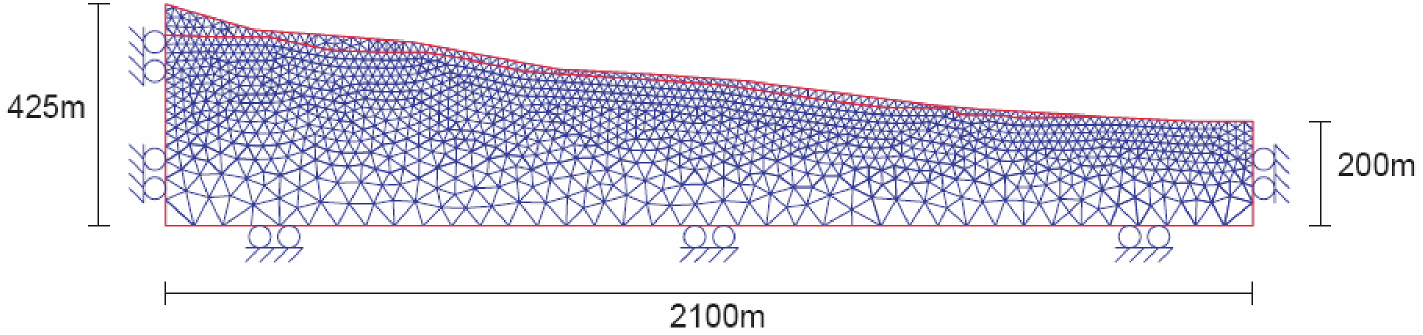

Finite element mesh of the Petacciato coastal slope

- Van Eekelen yield criterion :

$$\boxed{f = I_{2\sigma} + m\left(I_\sigma - \frac{3c}{\tan\varphi_c}\right) = 0}$$

  - With : $m = a(1 + b\sin 3\varphi)^n$

$$b = \frac{\left(\dfrac{r_c}{r_e}\right)^{\frac{1}{n}} - 1}{\left(\dfrac{r_c}{r_e}\right)^{\frac{1}{n}} + 1} \qquad a = \frac{r_c}{(1+b)^n}$$

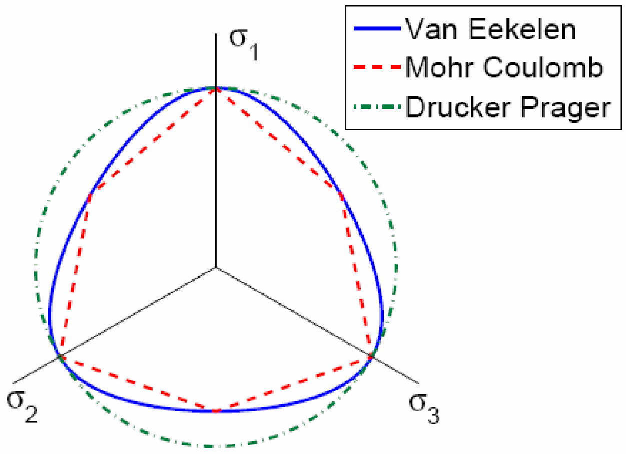

$$r_c = \frac{2\sin\varphi_c}{\sqrt{3}(3-\sin\varphi_c)} \qquad r_e = \frac{2\sin\varphi_e}{\sqrt{3}(3+\sin\varphi_e)}$$

$$\boxed{n = -0.229}$$

- evolution of the internal variables :
  - hyperbolic function of :

$$\varepsilon_{eq}^{p} = \int_0^t \dot{\varepsilon}_{eq}^{p} dt = \int_0^t \sqrt{\frac{2}{3} tr(\underline{\dot{e}})^2}\, dt$$

$$\underline{\dot{e}} = \underline{\dot{\varepsilon}}^{p} - \frac{tr(\underline{\dot{\varepsilon}}^{p})}{3}\underline{1}$$

  - Internal variables :

$$\varphi_c = \varphi_{c0} + \frac{(\varphi_{cf} - \varphi_{c0})\varepsilon_{eq}^{p}}{B_p + \varepsilon_{eq}^{p}}$$

$$\varphi_e = \varphi_{e0} + \frac{(\varphi_{ef} - \varphi_{e0})\varepsilon_{eq}^{p}}{B_p + \varepsilon_{eq}^{p}}$$

$$c = c_0 + \frac{(c_f - c_0)\varepsilon_{eq}^{p}}{B_c + \varepsilon_{eq}^{p}}$$

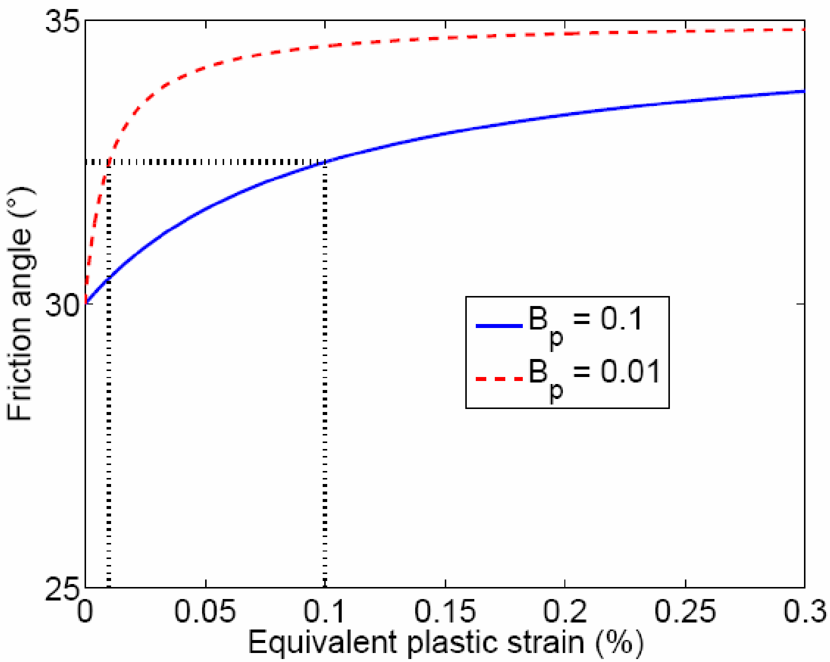

$$(\varphi_0 = 30°, \varphi_f = 35°)$$

Trévoux soil parameters

Soil parameters	Unit	Upper fill (1)	Low fill (2)	Sand clay (3)	Gravelly sand (4)	Gravelly marl (5)	Compact marl (6)
Grain specific weight	kN/m^3	26.	26.	29.00	28.00	27.	28.5
Young modulus	MPa	38.6	38.6	30.0	20.0	46.3	100.0
Poisson's ratio	-	0.29	0.29	0.29	0.29	0.29	0.29
Porosity	-	0.3	0.3	0.5	0.5	0.3	0.3
Intrinsic permeability	m^2	10^{-10}	10^{-10}	10^{-10}	10^{-10}	10^{-14}	10^{-14}
Initial friction angle	°	10.0	10.0	10.0	10.0	35.0	35.0
Final friction angle	°	35.0	35.0	35.0	40.0	35.0	35.0
B_p coefficient	-	0.008	0.008	0.008	0.008	0.008	0.008
Cohesion	kPa	10.0	15.0	1.0	1.0	100.0	100.0
Dilatancy angle	°	0	0	3.2	3.2	2.0	2.0

Petacciato soil parameters

Soil parameters	Symbols	Unit	Blue-gray clay
Grain specific weight	ρ_s	kN/m^3	27.
Young modulus	E	MPa	95.0
Poisson's ratio	ν	-	0.21
Porosity	n	-	0.3
Intrinsic permeability	k_w	M^2	10^{-17}
Initial friction angle	φ_0	°	1.0
Final friction angle	φ_f	°	19.0
B_p coefficient	B_p	-	0.01
Initial cohesion	c_0	kPa	10
Final cohesion	c_f	kPa	171
B_c coefficient	B_c	-	0.02
Dilatancy angle	$\psi_0 = \psi_f$	°	0

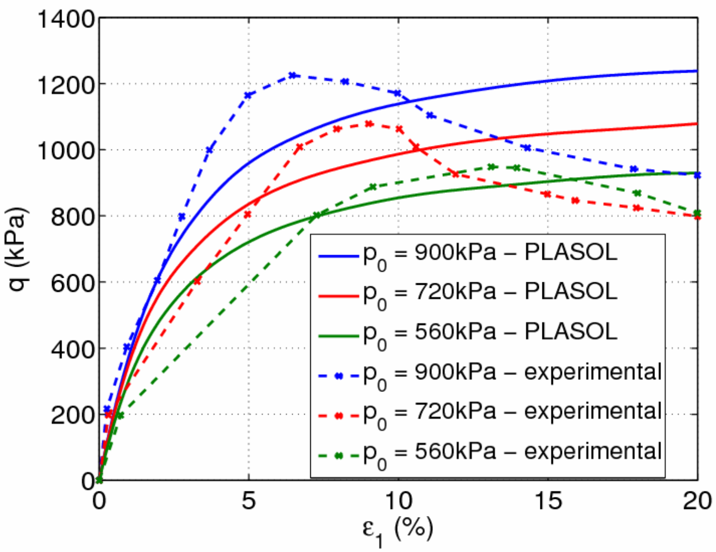

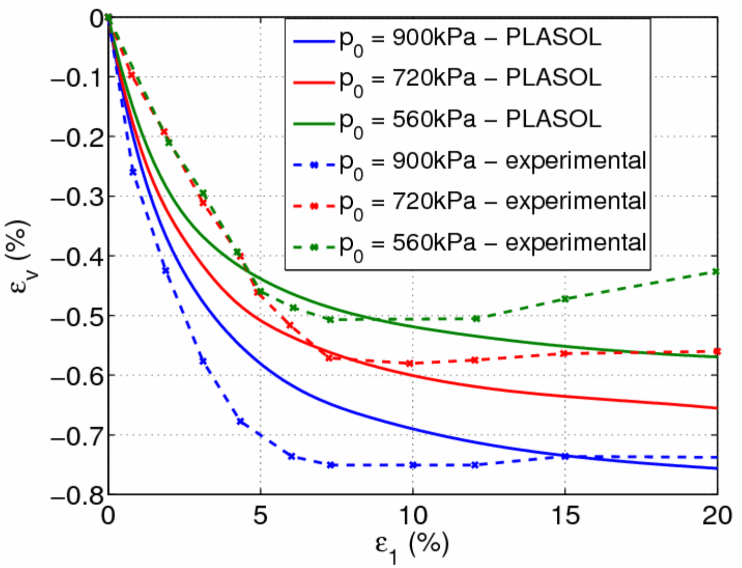

- Time dependent model of water transfer :
  - Pressure head : $$h_w = \frac{p_w}{\gamma_w} + y$$
  - Generalised Darcy's law : $\underline{v}_w = -K_w\left(p_c\right)\underline{\nabla} h_w$
  - Richard's equation : $\boxed{\frac{\partial \theta_w}{\partial t} = \underline{\nabla}^T\left(K_w(p_c)\underline{\nabla} h_w\right)}$ (Darcy + water mass balance)

With $\theta_w = nS_{ew}$ (volume water content)

and $$S_{ew} = \left(\frac{V_w}{V_v}\right)_{current}$$

- Richards equation depends on 2 hydrodynamic characteristics :
  - Water retention curve of Van-Genuchten :

$$S_{ew} = S_w + \frac{S_w - S_{rw}}{\left(1 + (\alpha p_c)^\beta\right)^{1-1/\beta}} \qquad S_{rw} = \left(\frac{V_w}{V_v}\right)_{\text{minimal}} \qquad S_w = \left(\frac{V_w}{V_v}\right)_{\text{maximall}}$$

  - Permeability : $K_w = S_{ew} k_w$

- Effective stress : $\underline{\sigma}' = \underline{\sigma} - p_a \underline{1} + \chi (p_a - p_w) \underline{1}$

With : $\chi = S_{ew}$

Water retention curve for Trévoux

Parameters	Symbols	Unit	Sands	Marls
Maximal degree of saturation	S_w	-	1.0	1.0
Residual degree of saturation	S_{rw}	-	0.1	0.1
First retention parameter	α	Pa^{-1}	$6.8\ 10^{-5}$	$2.5\ 10^{-5}$
Second retention parameter	β	-	4.8	2.0

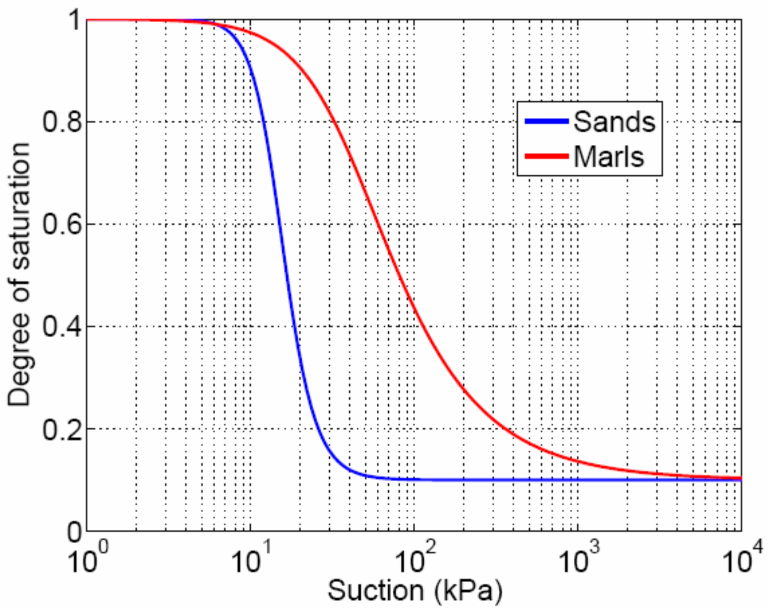

Water retention curve for Petacciato

Parameters	Symbols	Unit	Clay
Maximal degree of saturation	S_w	-	1.0
Residual degree of saturation	S_{rw}	-	0.1
First retention parameter	α	Pa^{-1}	$1.0\ 10^{-5}$
Second retention parameter	β	-	1.35

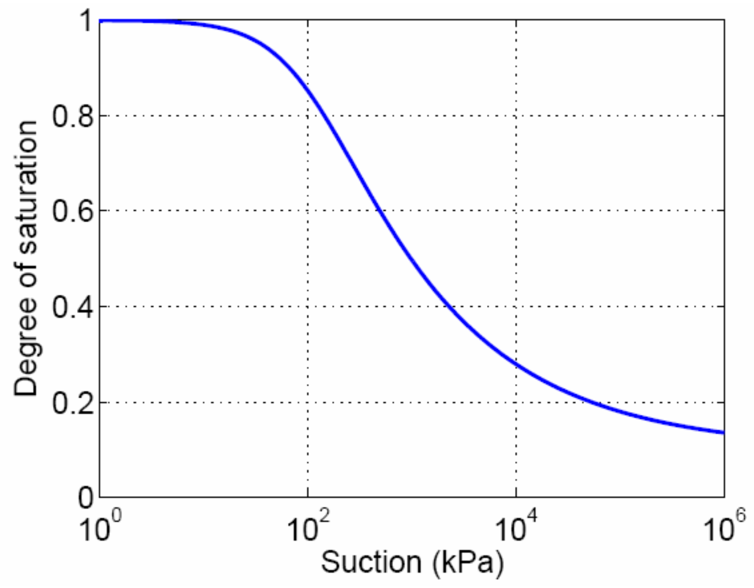

Implementation of d^2W in finite element code Lagamine

- Expression of Hill's stability criterion :
  - Local second order work : $d^2W_{pi} = d\underline{\sigma}'_{pi} : d\underline{\varepsilon}_{pi}$

normalised : $d^2W_{norm.} = \dfrac{d^2W_{pi}}{\|d\underline{\sigma}'\|_{pi}\|d\underline{\varepsilon}\|_{pi}}$

  - Global second order work : $D^2W = \sum_{pi=1}^{N_{pi}} d\underline{\sigma}'_{pi} : d\underline{\varepsilon}_{pi} . \omega_{pi} J_{pi}$

normalised, weighted : $D^2W_{norm.} = \dfrac{D^2W}{\sum_{pi=1}^{N_{pi}} \omega_{pi} J_{pi} \sum_{pi=1}^{N_{pi}} \|d\underline{\sigma}'\|_{pi}\|d\underline{\varepsilon}\|_{pi}}$

with :

N_{pi} : total number of integration points

J_{pi} : determinant of Jacobian transformation matrix for point *pi*

ω_{pi}: weight factor for point *pi*

Application to landslides

- Loading program in the simulation :
  - Initial state: unsaturated soil (dry)
  - Progressive saturation by increasing the water table
  - Stability analysis thanks to second order work criterion
- Results :
  - Iso values of the second order work
  - Global second order work of the problem vs loading parameter

- Evolution of local second order work
  - Water rising modelling

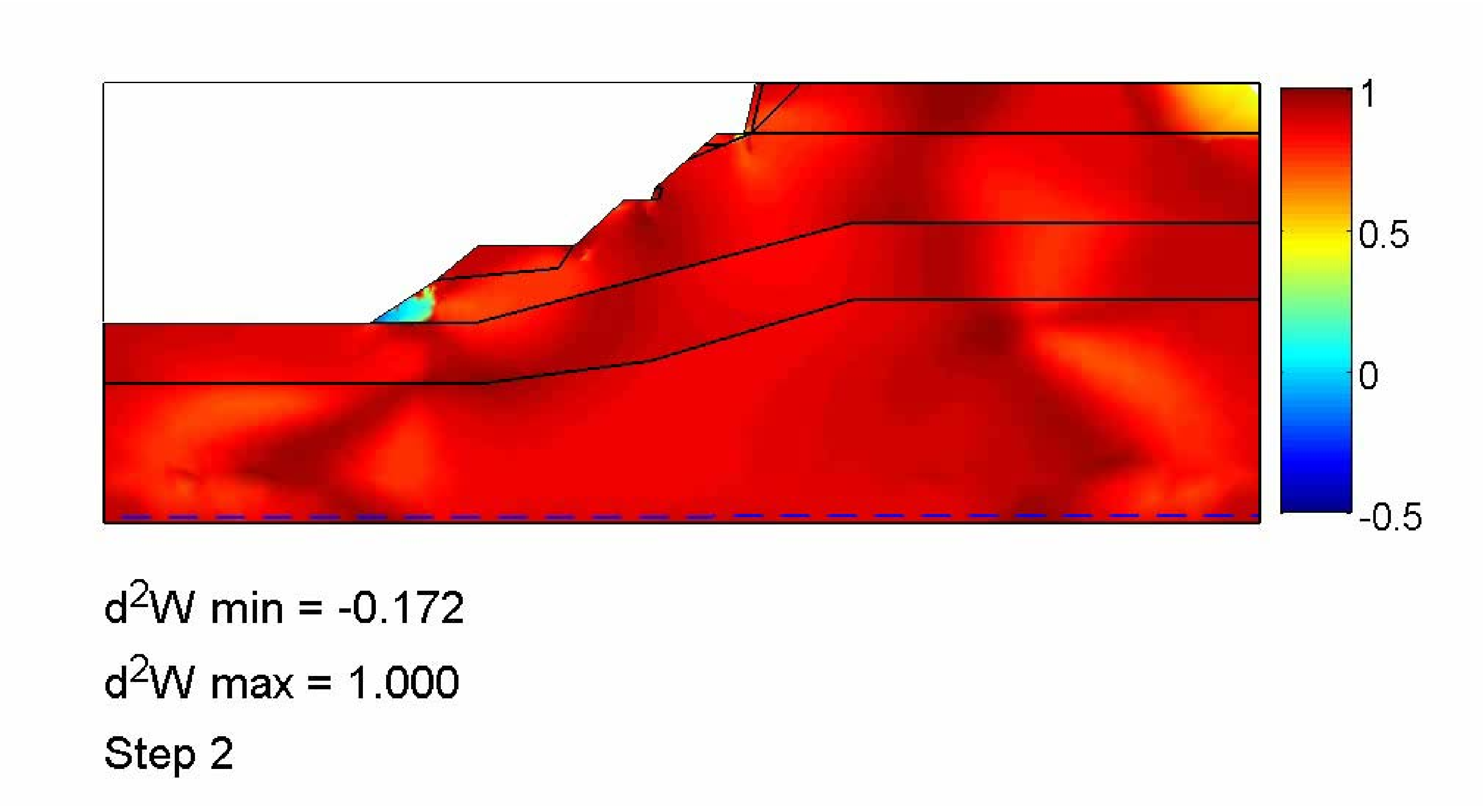

- Evolution of local second order work
  - Water rising modelling

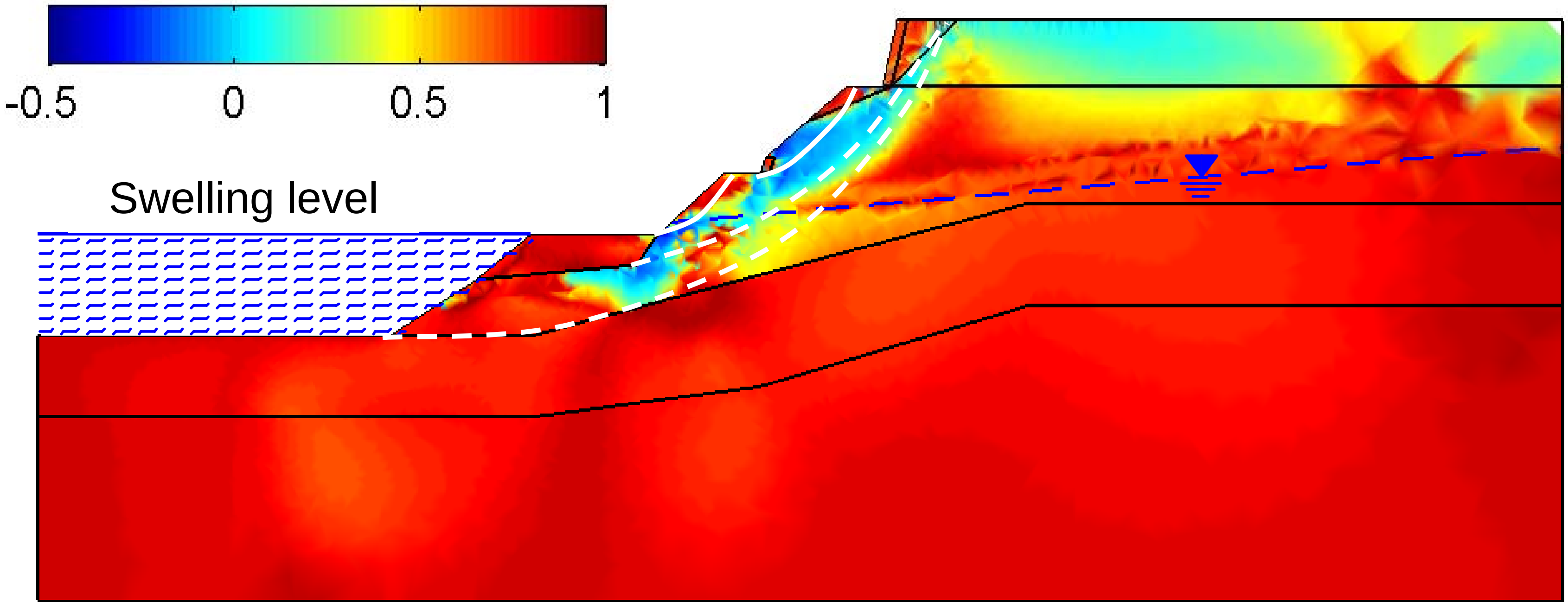

- Evolution of global second order work :

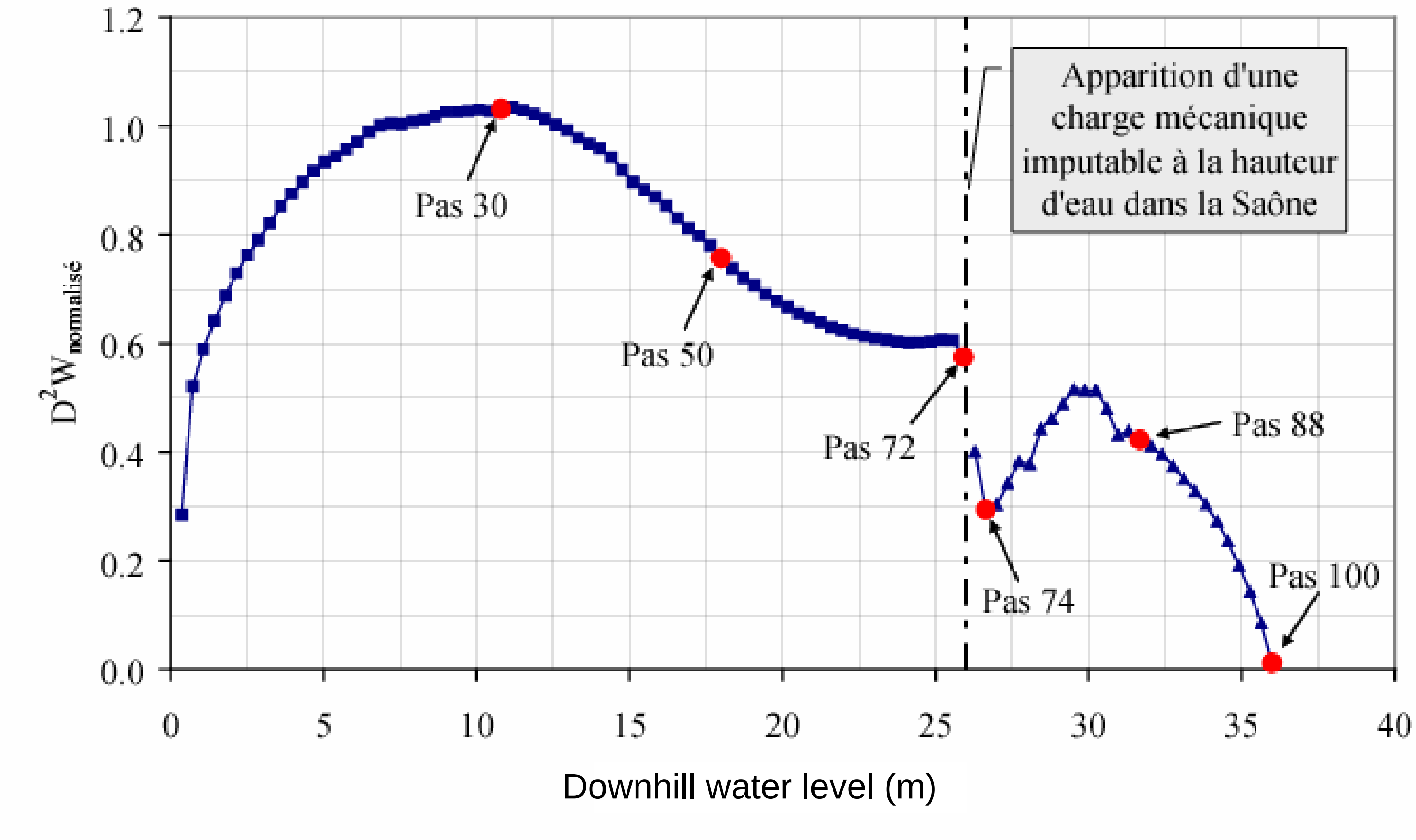

- Evolution of local second order work
  - Water rising modelling

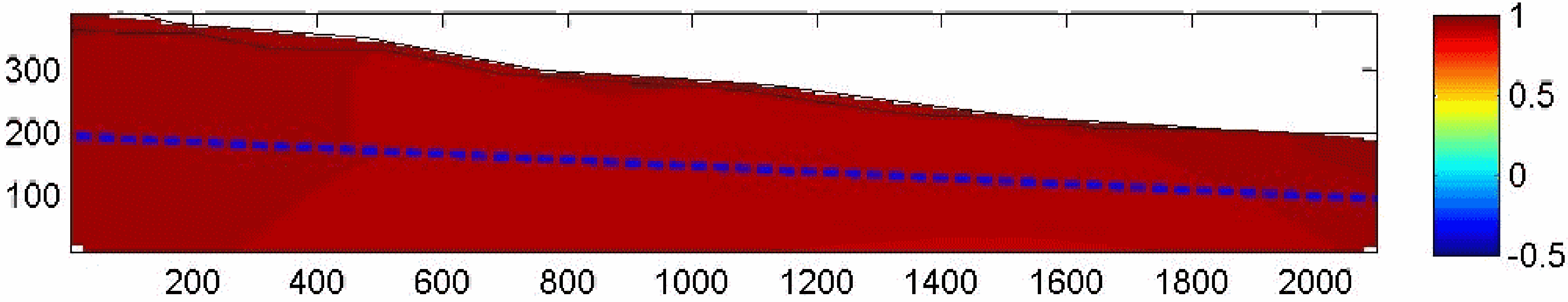

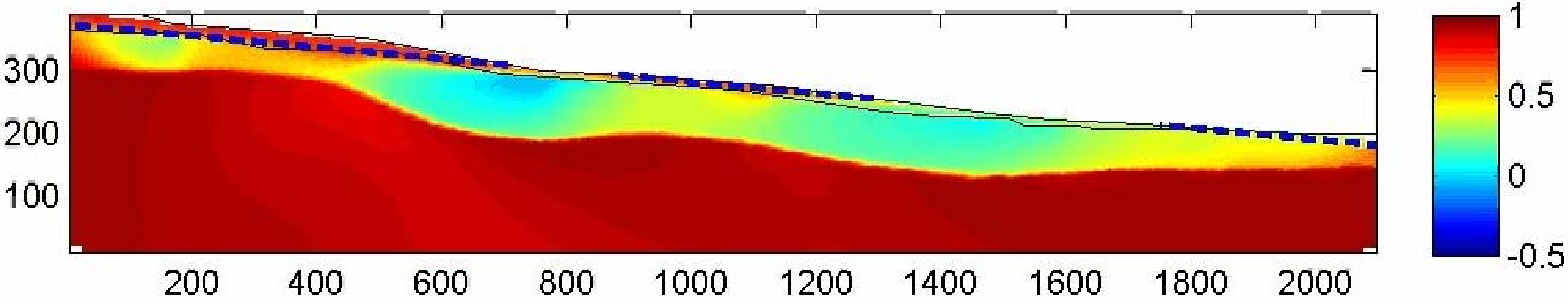

- Evolution of global second order work :

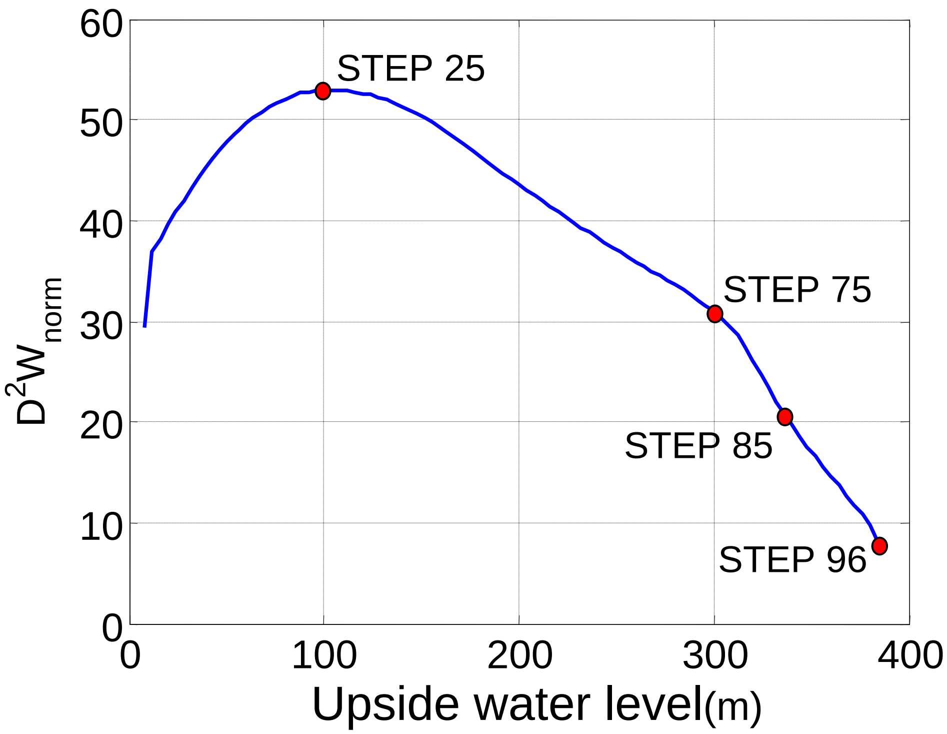

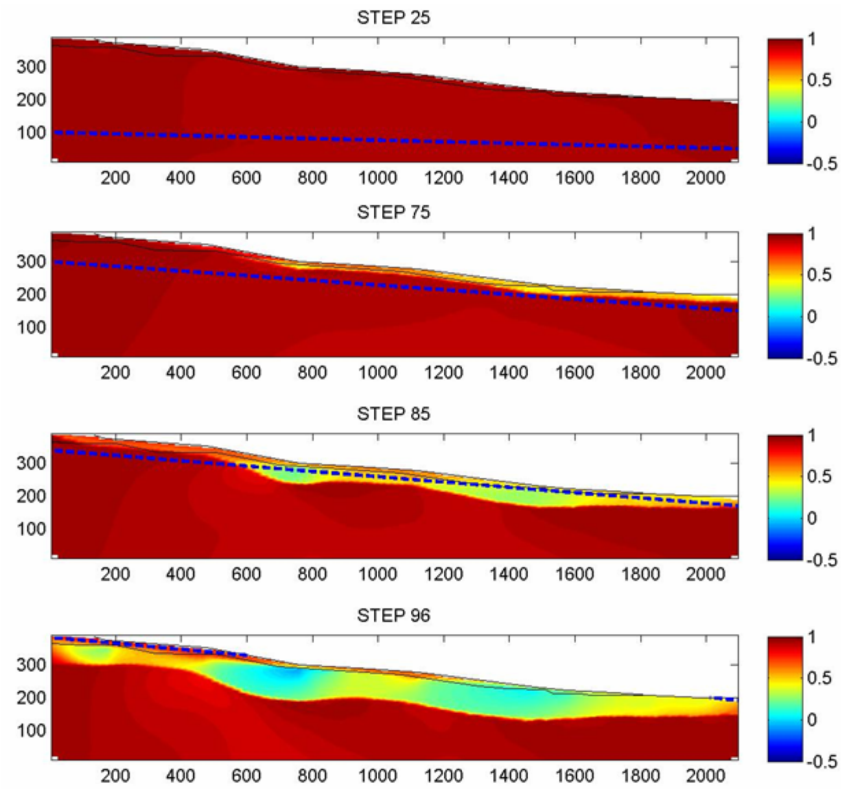

CONCLUSIONS

- Locally, **Hill's bifurcation criterion** comes before the other criteria (i.e. Mohr-Coulomb plastic limit condition, Rice's localisation condition, etc.).
- Application of **Hill's criterion** to stability analyses of non-linear boundary problems :
  - Material scale : local second order work criterion
    - detection of different failure modes (localized, diffuse),
    - description of the propagation of the potentially unstable zones.
  - Global scale : global criterion by integrating of local second order work into considered volume
    - description of global stability of the whole body,
    - highlight of the influence of the parameters of the constitutive behaviour (saturation, hydraulic conductivity, etc.) and events of hydraulic nature (raining, water flow, earthquakes, etc.) or anthropic (constructions, excavations, etc.) to the global stability of body.